The ClpP peptidase grips a model protein substrate against external force

By

Steven Dee Walker

Dissertation

Submitted to the Faculty of the

Graduate School of Vanderbilt University

in partial fulfillment of the requirements

for the degree of

DOCTOR OF PHILOSOPHY

in

Chemical and Physical Biology

December 17, 2022

Nashville, TN

Approved:

Breann Brown, Ph.D., Chair

Matthew Lang, Ph.D.

Gregor Neuert, Ph.D.

Houra Merrikh, Ph.D.

Marija Zanic, Ph.D.

Dedication

To my grandfather, Dr. Dee Walker, scientist and pioneer

Acknowledgements

This work was only possible due to the support and training I received from the Molecular Biophysics Training Program, Vanderbilt's Biochemistry program, and the chemical and physical biology program. I am very grateful for my mentor, Dr. Adrian Olivares, who supported me throughout my entire PhD, through a global pandemic, and has always inspired me to pursue whatever career interests I had. Thank you to all these people/groups for making my time at Vanderbilt University productive and joyful.

Who would a person be without a group of friends supporting them? I would like to thank my close friends who started their Ph.D. candidacy at the same time as me, especially Joseph Cleland, Lee Cantrell, Alexandra Schwartz, and Jason Hughes. Your support, endless science conversations, and fun times helped graduate school be an enjoyable experience for me. I wish you all the best of luck in your future endeavors.

I would like to acknowledge my wonderful family and their support through this time. My parents have always supported me throughout my endless years of schooling, offered guidance through difficult decisions, and are the two best role models I could ask for. My five siblings, for providing friendly competition and open ears when I needed them most. Hopefully I will soon be joining three of you as doctors (but not that kind). And to my in-laws, nieces, and nephews for making holidays feel exciting and fun.

Finally, I would like to thank my loving partner, David Brownlee, for inspiring me and helping me be the best person I can be. I would not have made it this far without your continued support and hope we continue for many years to come.

Table of Contents

Page

List of Tables

Table **Page**

List of Figures

Figure **Page**

CHAPTER 1

Introduction

Protein degradation is an essential process for the proteostasis network in all cells. Through various protein degradation pathways, cells remove damaged proteins, maintain appropriate protein expression levels, and control stages of the cell cycle. Furthermore, the dysregulation and/or breakdown of the proteostasis network contributes to aging (Hipp et al., 2019; Klaips et al., 2017) and various neurodegenerative diseases such as Alzheimer's and Parkinson's disease (Kurtishi et al., 2019). Therefore, understanding the basic biology of protein degradation pathways may provide new insights into mechanisms of such diseases and how to better treat them.

1.1 The importance of ClpP as the peptidase component of a AAA+ machine

One type of degradation machinery within the proteostasis network are AAA+ (ATPases Associated with diverse cellular Activities) proteases, which power protein degradation in the cell to eliminate damaged or misfolded proteins and modulate protein expression levels. These proteolytic molecular machines comprise ATP-dependent, ring-shaped motor proteins (i.e. AAA+ protein unfoldases) that recognize, unfold and translocate substrate protein into a self-compartmentalized peptidase (Olivares et al., 2015, 2018). Caseinolytic peptidase P, ClpP, is the peptidase component of a AAA+ protease that associates with the ClpA, ClpX, and ClpC motors (Maurizi, Clark, Kim, et al., 1990; Yu & Houry, 2007). ClpP is a canonical serine protease with a Ser-His-Asp catalytic triad, though its fold is unique from other families (Maurizi, Clark, Katayama, et al., 1990; Maurizi, Clark, Kim, et al., 1990; Yu & Houry, 2007). ClpP homologs are found in prokaryotes as well as the mitochondria and chloroplasts of eukaryotic cells. In prokaryotes, ClpP

is necessary for cell cycle control (Jenal & Fuchs, 1998), protein turnover (Kock et al., 2004), and pathogenesis in specific organisms like *Staphylococcus aureus* and *Listeria monocytogenes* (Bhandari et al., 2018; Gaillot et al., 2000). Additionally, in humans ClpP mutants cause Perrault syndrome (Brodie et al., 2018; Jenkinson et al., 2013), classified by female infertility and sensorineural hearing loss. Thus, understanding ClpP function impacts human health in several areas, though this dissertation will focus on prokaryotic ClpP and its associated ClpA and ClpX unfoldases.

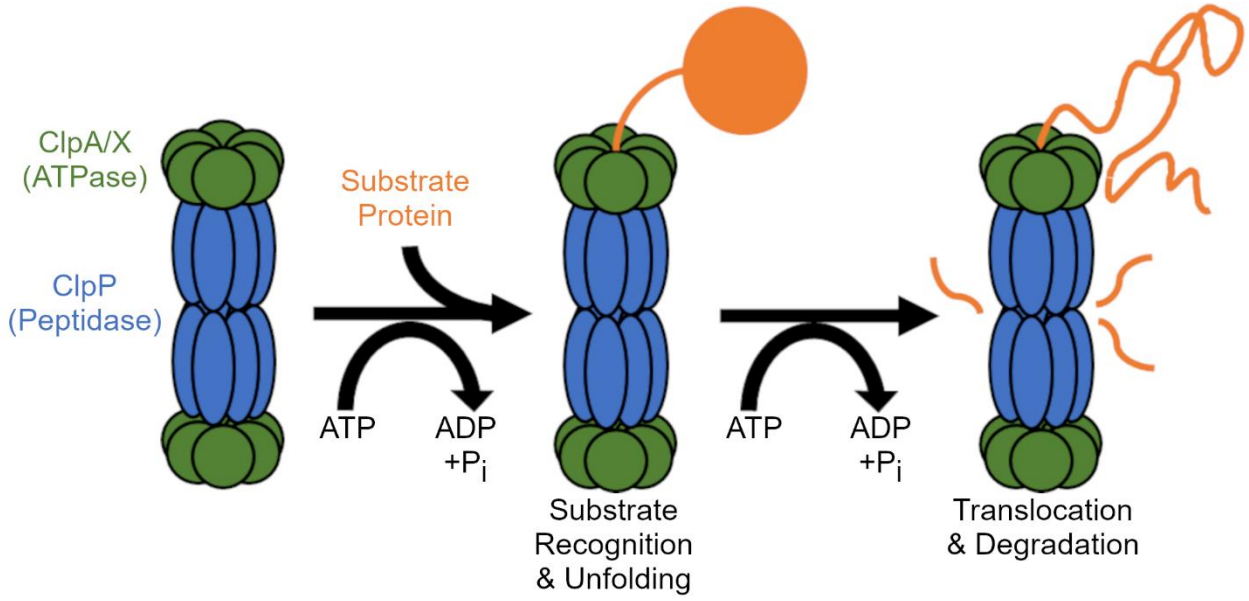

Figure 1.1 Established model of degradation by AAA+ proteases. ClpP (blue) binds to AAA+ motors on either end (green). These motors recognize protein (orange) and hydrolyze ATP to unfold them and translocate the polypeptide into ClpP for degradation.

To prevent indiscriminate proteolysis in cells, ClpP conceals its active sites within a central chamber, which are made accessible upon activation by binding AAA+ motors (Figure 1.1). The AAA+ motors in these complexes recognize tagged substrates (Burton et al., 2001; Flynn et al., 2003), provide energy through ATP hydrolysis (Olivares et al., 2018), and perform work to unfold protein substrates and thread them into ClpP for degradation (Sen et al., 2013). Several recent structures of the ClpXP and ClpAP complexes obtained by cryo-EM highlight these activities; additionally, they show how motor binding activates ClpP (Fei et al., 2020; Lopez et al., 2020; Ripstein et al., 2020). AAA+ unfoldase binding activates ClpP by opening the axial pore through

rearrangement of its N-terminal loops, allowing polypeptide to be threaded into the ClpP chamber for degradation. These N-terminal loops are responsible for substrate gating in the absence of motor proteins (Jennings et al., 2008; M. E. Lee et al., 2010), and have been shown to make important contacts with motor proteins (Fei et al., 2020; Ripstein et al., 2020). On its own, ClpP has been captured in three unique structural conformations that also feature rearrangement of these loops (Ye et al., 2013; Zhang et al., 2011). However, it remains unclear if ClpP populates all these conformations upon activation or if it is locked into the active state.

1.2 Previous evidence of mechanical contributions by ClpP

Many single molecule studies in the past decade have focused on how the AAA+ proteases ClpXP and ClpAP work together to unfold, translocate, and degrade protein substrates. More specifically, optical trapping experiments combined with solution biochemistry revealed how AAA+ proteases generate force, coordinate ATPase cycles, grip the protein substrate, and translocate along the polypeptide track (M.-E. Aubin-Tam et al., 2011; Cordova et al., 2014; Iosefson, Nager, et al., 2015; Iosefson, Olivares, et al., 2015; Kotamarthi et al., 2020; Maillard et al., 2011; Olivares et al., 2014, 2017; Rodriguez-Aliaga et al., 2016; Sen et al., 2013). These force dependent phenomena are fundamental to the biological function of these molecular machines. ATP hydrolysis by the AAA+ motors is directly coupled to protein unfolding and translocation (Kenniston et al., 2003; Martin et al., 2008). Since the AAA+ motors hydrolyze ATP to perform work, ClpP has been overlooked as a possible contributor to the chemomechanical cycle of the AAA+ machines. However, there is evidence in literature which shows ClpP binding and activity affect its motor partners biochemically and mechanically. For example, ClpP binding causes ClpA to take faster kinetic steps (Miller et al., 2013; Rajendar & Lucius, 2010) and unfold a dimeric protein substrate more quickly (Baytshtok et al., 2015). Furthermore, ClpP binding to ClpX reduces the size and frequency of backslipping (M.-E. Aubin-Tam et al., 2011; Iosefson, Olivares,

et al., 2015; Maillard et al., 2011). Although these phenomena can be partially explained by changes in ATPase rates upon ClpP binding (i.e. increasing for ClpA and slightly decreasing for ClpX) (Hinnerwisch et al., 2005; Kim et al., 2001), there is still a gap in understanding what features in ClpP may contribute these mechanical activities.

In addition to motor proteins, ClpP is also activated by a class of natural products called acyldepsipeptides (ADEPs) (Brötz-Oesterhelt et al., 2005; Malik & Brötz-Oesterhelt, 2017). Structurally, ADEPs comprise three important features: a lactone core made of modified amino acids, a phenylalanine linker, and an acyl tail (B.-G. Lee et al., 2010). ADEPs bind to the same hydrophobic pocket on ClpP to which motors bind (Amor et al., 2016) and are thought to activate ClpP in a similar manner, i.e., by causing rearrangement of the ClpP N-terminal loops (Gersch et al., 2015). In cells, ClpP activation by ADEPs leads to cell death through the indiscriminate proteolysis of nascent polypeptides and metastable protein substrates (Brötz-Oesterhelt et al., 2005). Thus, ADEPs show promise as antibiotics against biofilms in mice (Conlon et al., 2013) and as anticancer therapies due to ClpP's conserved role in mitochondrial proteostasis (Graves et al., 2019) (further reviewed in (Bhandari et al., 2018; Moreno-cinos et al., 2019; Wong & Houry, 2019; Ye et al., 2017)). In bacteria, ADEP activation inhibits cell division through the specific degradation of FtsZ (Sass et al., 2011), which forms the Z-ring during cytokinesis. Furthermore, using purified components *in vitro*, Silber and colleagues showed that ADEP-activated ClpP unfolds and degrades FtsZ without a motor protein (Silber et al., 2020), suggesting that activated ClpP might possess similar mechanical unfoldase and translocase activities as its partner motor proteins.

Here I provide a review of 3 different areas of ClpP mechanobiology. First, I analyze the historical context of ClpP structures highlighting several key conformations it occupies. Next, I assess the activation mechanism of ClpP in the context of motor proteins and ADEPs. Finally, I review the single molecule mechanics of the ClpXP and ClpAP complexes showing areas where ClpP activity may contribute mechanically.

1.3 Structures of the ClpP monomer and tetradecamer

The first structure of *Escherichia coli* ClpP (EcClpP) was determined using X-ray crystallography by Wang, Hartling, and Flanagan in 1997 (Wang et al., 1997). They found that ClpP had a unique fold comprising six α/β repeats "resembling a hatchet" with two domains they called the head and the handle (Figure 1.2A). They showed that ClpP assembled into tetradecamers, two heptameric rings stacked with the handle domains responsible for heptamer-heptamer contacts. The catalytic triad residues were sequestered near a cleft between the head and handle domains. Importantly, the catalytic triad was located at the interface between monomers, suggesting that oligomerization is necessary for degradation. In fact, not only EcClpP relies on oligomerization for degradation activity, but *S. aureus* (SaClpP) (Gersch et al., 2012), *Homo sapiens* (HsClpP) (Brodie et al., 2018), and *Mycobacterium tuberculosis* (MtClpP) (Schmitz et al., 2014) require oligomerization for degradation. Finally, Wang et al. hypothesized that the size of the central pore would determine the size of peptide entry and modeled a hepta-peptide substrate binding the substrate cleft of ClpP. This has since been supported structurally and biochemically as it has since been shown that ClpP gating relies on its N-terminal loops to open or occlude its central pore (Effantin et al., 2010; Gribun et al., 2005; Jennings et al., 2008; M. E. Lee et al., 2010).

After this initial ClpP structure, several groups determined structures of ClpP from prokaryotes that were captured in different conformations. ClpP from *Streptococcus pneumoniae* (Gribun et al., 2005) with a single point mutation (SpClpPA153P) and *Mycobacterium tuberculosis* (Ingvarsson et al., 2007) were captured in a "compressed" conformation. Following these studies, SaClpP (Geiger et al., 2011; Ye et al., 2013; Zhang et al., 2011) and a disulfide crosslinked variant of EcClpP (Kimber et al., 2010) were also captured in similar compressed conformations. In comparison to the original "extended" conformation, the compressed state features a kink in the

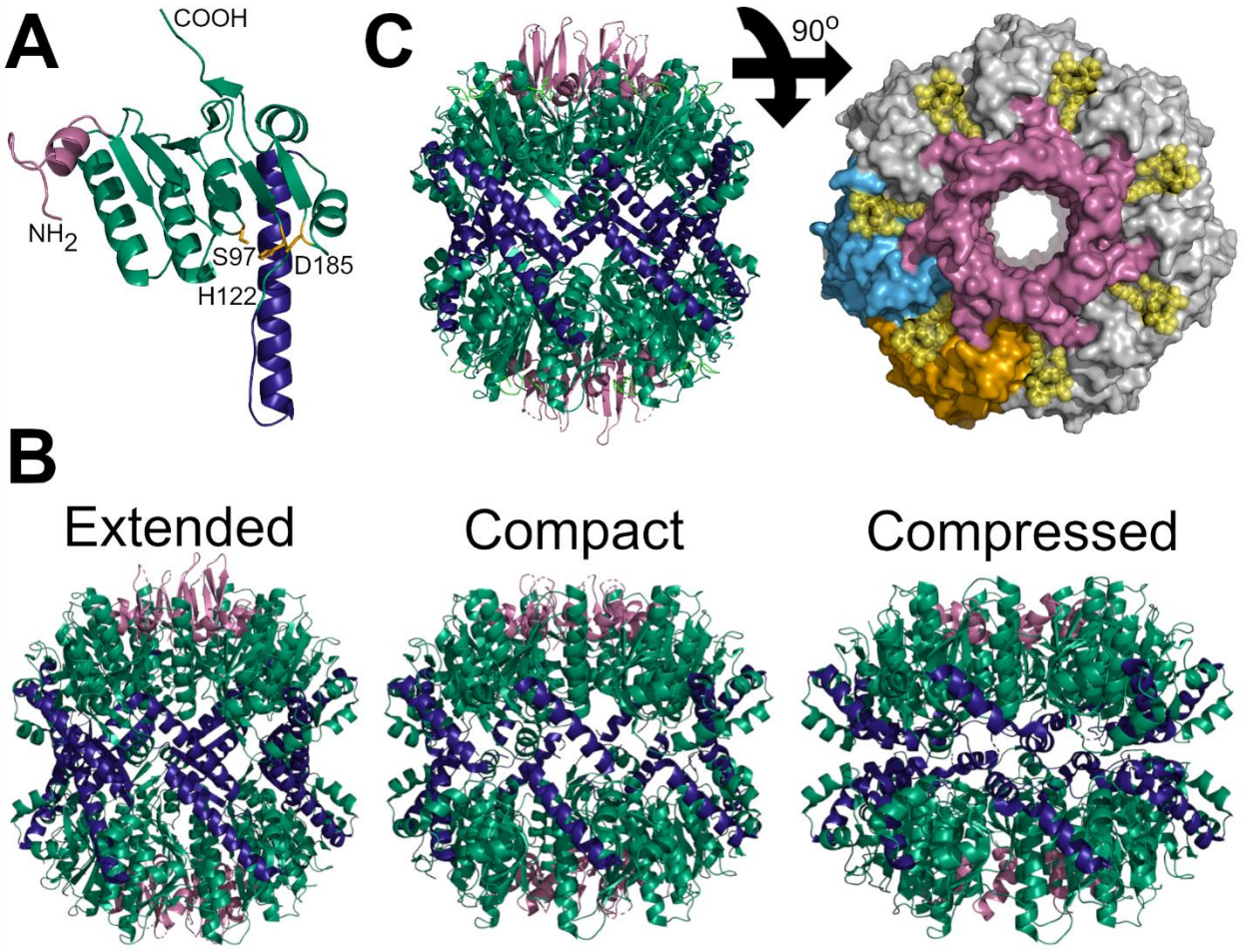

Figure 1.2 Conformational dynamics of ClpP (A) Structure of the EcClpP monomer (PDB: 1TYF). The structure is divided into two regions: the handle (Violet) and head (teal). The N-terminal residues are colored pink. The residues of the catalytic triad are colored yellow and labeled. (B) Structures of SaClpP in three unique conformations (PDB: 3STA, 4EMM, 3ST9 from left to right). Coloring is the same as in A. The N terminal loops form ordered β-hairpins in the extended and are disordered in the compact and compressed conformations. The handle α-helix kinks in the compressed conformation. (C) Structure of EcClpP bound to ADEP1 (PDB: 3MT6). Left: Cartoon showing a side view of the ClpP tetradecamer, coloring is the same as in A. Right: Space filling model showing a top-down view of ClpP. The N-terminal loops are colored pink, and two adjacent monomers are colored cyan and orange for viewing. ADEP1 is colored yellow and binds within the hydrophobic pocket between monomers.

handle domain α-helix (Geiger et al., 2011; Ye et al., 2013; Zhang et al., 2011) resulting in a 10 angstrom compaction of the height of the tetradecamer (Figure 1.2B). These conformational changes also disrupt the catalytic triad geometry rendering such conformations inactive. The α-helix kink creates an opening along the equator of the ClpP tetradecamer, which is thought to

allow peptides to exit the central chamber. This is supported by an NMR study of crosslinked EcClpP which captured substrates when crosslinked and released products when reduced (Sprangers et al., 2005). Additionally, chemically inactivated ClpXP released a captured GFP substrate upon addition of ATP and excess substrate (Kim et al., 2000), suggesting polypeptide egress outside a different opening than the central pore. Taken together, these studies support the idea that ClpP must occupy the compressed conformation to allow peptide release after proteolysis.

1.4 ClpP conformational cycling

Does wild type ClpP cycle between these conformations in solution? While it is still unclear, several studies support the idea that ClpP switches between these conformations during proteolysis. Normal mode analysis comparing wild type and crosslinked EcClpP suggests that wild type ClpP samples the compressed conformation (Kimber et al., 2010). Furthermore, wild type SaClpP has been captured in both extended and compressed conformations *in crystallo* (Figure 1.2B) (Geiger et al., 2011; Zhang et al., 2011). In addition, molecular dynamics simulations of SaClpP structures find a third “compatct” state (Ye et al., 2013), which might represent an intermediate between extended and compressed. This theoretical structure was also crystallized by Ye et al. and found to be similar to the SpClpPA153P structure (Sprangers et al., 2005). They suggest that Ala140 in *S. aureus*, which is Ala140 in *E. coli* and *S. pneumoniae*, act as the hinge during the transition from extended to compressed. Taken together, these structures suggest that ClpP is capable of cycling through conformations in solution, and that it might be necessary for product release. However, more evidence is needed to definitively conclude if ClpP does cycle between conformations during degradation, and how that would affect its function in complex with motor proteins.

With respect to motor proteins, three different structures of the ClpXP and ClpAP complexes were recently determined by cryo-EM: one for EcClpXP (Fei et al., 2020), EcClpAP (Lopez et al., 2020), and *Neisseria meningitidis* ClpXP(Ripstein et al., 2020) (For recent reviews of motor protein structures see (Gates & Martin, 2020; Mabanglo & Houry, 2022)). In all three structures, motor bound ClpP is found in the extended conformation. Furthermore, for the EcClpAP structure, data sets with singly capped ClpP were also analyzed (i.e., where ClpA is bound to one heptamer of the ClpP tetradecamer). In this case, the ClpP heptamer bound to ClpA was in the extended conformation while the unbound ClpP heptamer featured a closed central pore (Figure 1.3A). The presence of a closed pore suggests a compressed/compact conformation for ClpP; however, Lopez et al. did not perform this comparison directly. Finally, while all three studies had substrate present in their experiments, there was either too little or no density within ClpP to suggest a method of substrate engagement. Perhaps future studies with inactive variants of ClpP and motors will be able to capture substrate within the central chamber, giving a more complete picture of how both proteins contribute to substrate engagement for the ClpAP and ClpXP machines.

1.5 The importance of ClpP's N-terminal loops

Within the ClpP conformational landscape, the N-terminal loops have been a point of controversy between structures. For this review, the N-terminus generally comprises the first 20 amino acids of the mature ClpP monomer. These residues are important for efficient degradation as mutations in the pore-lining segments decrease substrate degradation rates (Alexopoulos et al., 2013). For the original 1997 structure (Wang et al., 1997), the density for the N-terminus was not strong enough to model, suggesting flexibility within the crystal structures. A later structure of SpClpP found that the N-terminal residues formed flexible β-hairpin loops, with residues 2-8 being too flexible to model, and further showed that these residues were important for motor protein

binding (Gribun et al., 2005). However, a higher resolution crystal structure later found the N-terminal loops in two conformations which they termed “up” and “down” (Bewley et al., 2006). In the up conformation, six of these loops in one heptamer adopt ordered β-hairpin conformations with unsatisfied hydrogen bonding towards the pore than could interact with entering substrate (Figures 1.2B and C show similar N-terminal loop structures). However, the N-terminal loops of the opposite heptamer were in the down conformation. In the down conformation, the density for residues 1-11 was too weak to model confidently, but density from residues 12 onward suggests it enters the central pore to bind ClpP within. Similarly, a chemically inactivated EcClpP crystal structure (Szyk & Maurizi, 2006) captured its N-terminal loops in several different conformations within the same crystal. Importantly, each of these authors noted that crystal contacts could influence the conformation of individual loops, partially explaining why different loops within the heptamer were captured in up or down conformations. Thus, from structures of ClpP alone it appears the N-terminal loops are flexible in solution occupying at least two distinct conformations.

The structures of activated ClpP provided a clearer picture regarding the N-terminal loops. Using ADEPs, two different groups initially captured crystal structures of activated *Bacillus subtilis* ClpP (BsClpP) (B.-G. Lee et al., 2010) and EcClpP (Li et al., 2010). In the BsClpP structure, ADEP binding increased the N-terminal loop flexibility, which could not be modeled, while also enlarging the central pore. In contrast, the activated EcClpP structure captured all N-terminal loops not participating in crystal contacts in an ordered β-hairpin (Figure 1.2C), reminiscent of the up conformation found previously (Bewley et al., 2006). Later, a crystal structure of ADEP bound to MtClpP also captured the N-terminal loops in the up conformation similar to EcClpP (Schmitz et al., 2014). Furthermore, all of the recent cryo-EM structures of ClpP with motor proteins (Fei et al., 2020; Lopez et al., 2020; Ripstein et al., 2020) found the N-terminal loops in ordered conformations similar to the ADEP-EcClpP structure (Figure 1.3A). For the ClpXP structures, these N-terminal loops also formed interactions with pore-2 loops residues in ClpX (Fei et al.,

2020; Ripstein et al., 2020). Taken together, it appears that the N-terminal loops of activated ClpP adopt an ordered “up” conformation, which is more difficult to capture using x-ray crystallography due to crystal packing artifacts. However, it is still possible that the N-terminal loops cycle between up and down in solution. In fact, the N-terminal loops of SaClpP (Geiger et al., 2011; Ye et al., 2013; Zhang et al., 2011) form the ordered “up” β-hairpins in the extended conformation and are disordered in the compact and compressed conformations (Figure 1.2B), which were all occupied during molecular dynamics simulations (Ye et al., 2013). Additionally, ADEP binding shifts the equilibrium of SaClpP toward the extended conformation in solution (Gersch et al., 2015). Overall, both the N-terminal loops and handle region of ClpP undergo structural rearrangements during activation and proteolysis, which may be important for degradation mechanics of ClpP on its own and in complex with motor proteins.

1.6 ClpP activation by AAA+ motors

On its own, ClpP only degrades small peptides due to gating by its N-terminal loops (Gribun et al., 2005; Jennings et al., 2008; M. E. Lee et al., 2010), which form a pore with an approximately 10 angstrom diameter in its inactive conformations (Bewley et al., 2006; Gribun et al., 2005; Kang et al., 2004; Kimber et al., 2010; Wang et al., 1997). Upon activation, this central pore opens to approximately 20 angstroms (Fei et al., 2020; B.-G. Lee et al., 2010; Li et al., 2010; Lopez et al., 2020; Ripstein et al., 2020) allowing unfolded substrates to enter for degradation (Figures 1.2C, 1.3A). Interestingly, even unique substrates like disulfide linked peptides (Burton et al., 2001), substrates with altered peptide bond spacing and unnatural side chains (Barkow et al., 2009), and knotted proteins (Martín et al., 2017; Sivertsson et al., 2019; Sriramoju et al., 2018) are degraded by activated ClpP. These features of activation are well explained by ClpP structural information, but what changes occur biochemically to ClpP and its motor proteins during

activation? Additionally, do motor proteins and ADEPs activate ClpP through similar or distinct mechanisms?

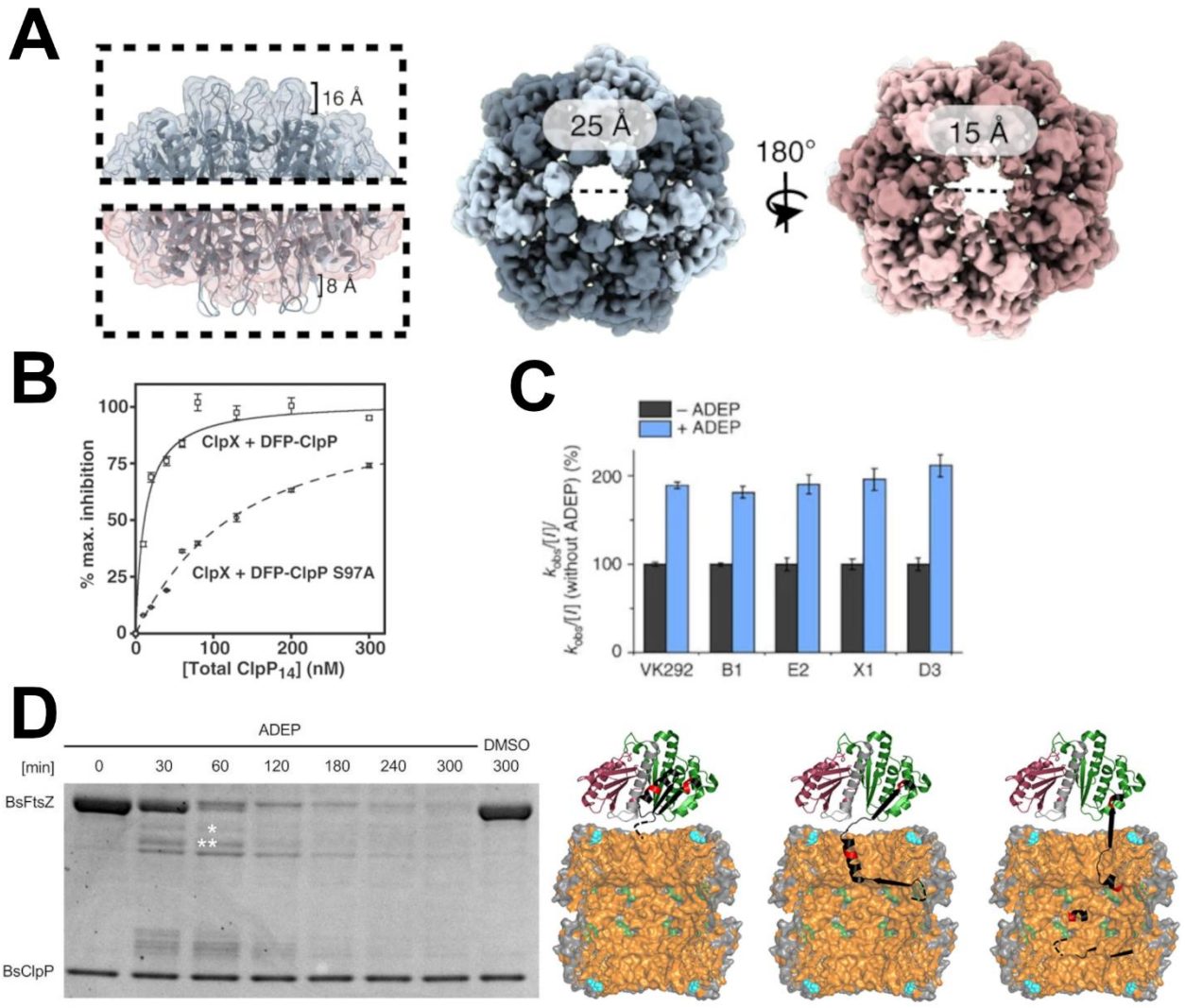

Figure 1.3 ClpP activation by AAA+ motors and ADEPs (A) Structures of single capped ClpP with hepatmers bound to ClpA (blue) and not bound (red). A Side view is shown on the left with top-down views on the right. Figures adapted from (Lopez et al. 2020). (B) ClpX ATPase inhibition by DFP-ClpP and ClpPS97A. K_{app} for DFP-ClpP was ≤5nM and was ~94nM for DFP-ClpPS97A. Figure adapted from (Joshi et al. 2004). (C) Catalytic efficiencies of SaClpP labeled with different β-lactones in the absence or presence of saturating ADEP7. The size of the β -lactones increases from left to right. Figure adapted from (Gersch et al. 2015). (D) (left) Time course of BsClpP degrading FtsZ *in vitro* with substoichiometric concentrations of ADEP. The starred bands were sequenced by Edman degradation and matched ClpP's N terminus. (right) Proposed model showing FtsZ entering the ClpP tetradecamer from a side view, with hydrophobic residues in orange. The hydrophobicity of the N terminus of FtsZ might allow ClpP to grip long enough for stoachastic unfolding and degradation. Figures adapted from (Silber et al. 2020).

I will begin by examining ClpP activation by motor proteins. Both ClpA and ClpX bind ClpP by docking hydrophobic IGL/F loops into the hydrophobic pocket of ClpP, which lies in the head region between monomers (Fei et al., 2020; Lopez et al., 2020; Ripstein et al., 2020). These interactions are highly dynamic and can be outcompeted by sub-stoichiometric amounts of ADEP (Amor et al., 2016). Motor protein binding only slightly decreases the peptide hydrolysis rate of ClpP for dipeptide substrates (Thompson et al., 1994). In contrast, ClpP binding slightly decreases the ATPase rate of ClpX and increases the ATPase rate of ClpA nearly two fold when degrading substrate (Baytshtok et al., 2015; Burton et al., 2001; Kenniston et al., 2003). This shows that ClpP binding affects the biochemical activity of the motor proteins, but motor binding does not affect ClpP's biochemical activity.

Interestingly, both ClpP and ClpX can "sense" the activity of the other protein. Joshi and colleagues (Joshi et al., 2004) showed this using various competitive degradation and ATPase assays. They found that ClpP has increased affinity for ClpX engaging a titin substrate; furthermore, they showed that ClpX binds chemically inactivated ClpP stronger than wild type or the active site serine to alanine mutant (Figure 1.3B). They reasoned that the presence of the acyl intermediate causes some change in ClpP that ClpX recognizes. This is possibly due to rearrangements of the N-terminal loops as seen in the chemically inactivated EcClpP structure (Szyk & Maurizi, 2006). This is also supported by a study of degradation by an N-terminal deletion of ClpP (ClpPΔN), which showed a slow phase of degradation due to a prolonged time spent with the acyl intermediate (Jennings et al., 2008). Taken together, these studies suggest a possible allosteric interaction between the N-terminal loops of ClpP and its active site hydrolysis activity. While both ClpP and motor proteins can sense the activity of their partner, only ClpP affects the biochemical activity of the ClpA and ClpX motors.

1.7 ClpP activation by ADEPs

How does activation by ADEPs affect ClpP biochemical activities? Similar to ClpA and ClpX binding, ADEP binding opens the central pore of ClpP to approximately 20 angstroms (B.-G. Lee et al., 2010; Li et al., 2010) allowing unfolded proteins to enter. Furthermore, ADEP binding does not increase the peptidase activity of ClpP against a dipeptide substrate (N-Succinyl-Leu-Tyr-7-amido-4-methylcoumarin) (Brötz-Oesterhelt et al., 2005; Li et al., 2010). However, this might not be true of all substrates for ClpP. In their study of SaClpP comparing ADEPs and motor proteins, Gersch and colleagues (Gersch et al., 2015) found that ADEP activation increased the labeling speed of ClpP by β-lactone inhibitors two fold (Figure 1.3C). This was true for the smallest lactone used, which had a maximum hydrodynamic diameter of approximately 7 angstroms, suggesting a mechanism independent of pore enlargement as it should fit into the non-activated ClpP pore. While ClpP activation by ADEPs may affect peptidase activity for certain substrates, to my knowledge no study has been done addressing β-lactone labeling of ClpP in the absence and presence of motors. Therefore, no direct comparison between ADEPs and motors can be made to address the increase in ClpP labeling speed by β-lactones by ADEPs. Overall, motor proteins and ADEPs appear to activate ClpP through similar mechanisms, by opening the central pore and allowing larger substrates to enter. It remains unclear if the peptidase activity is unchanged by ADEPs and motors, or if this activity is dependent on substrate properties.

In a cellular context, ClpP activation independent of motor proteins is detrimental to life. ADEP treatment of *B. subtilis* cells inhibits cell division (Brötz-Oesterhelt et al., 2005), leading to cell death, and treatment in mammalian cells leads to apoptosis (Wong et al., 2018) (For a review of HsClpP modulation (Wong & Houry, 2019)). Both of these activities are ClpP dependent and likely act through the same mechanism: the indiscriminate proteolysis of nascent and unfolded protein substrates in the cell (Kirstein et al., 2009). However, in *B. subtilis* cells ADEP-ClpP specifically degrades the cell division protein FtsZ (Sass et al., 2011). This activity is independent

of AAA+ motors as ClpX deletion strains still degraded FtsZ upon ADEP treatment (Sass et al., 2011). In cells, the degradation of FtsZ might also be influenced by other pathways that ADEP treatment could also be activating, such as the SOS response, which were not controlled for in this study. FtsZ forms the Z ring during cytokinesis to divide bacterial cells and has many protein partners to regulate its stability and polymerization (Romberg et al., 2017). *In vitro*, ADEP and ClpP are sufficient to degrade FtsZ (Sass et al., 2011), unfolding FtsZ in the process by its N terminus (Silber et al., 2020) (Figure 1.3D). It remains unclear how ADEP-ClpP unfolds this substrate and why FtsZ can be unfolded but not other protein substrates such as GFP (Kirstein et al., 2009). ADEP-ClpP also degrades α- and β-tubulin (Sass et al., 2011), suggesting it might be a conserved structure between the bacterial and mammalian cytoskeletal proteins that allows them to be degraded by ADEP-ClpP. However, more research is needed to determine the exact mechanism of unfolding and if it depends on certain structures in substrate proteins, biochemical stability, mechanical stability, or a combination of all these characteristics.

1.8 Implications of ClpP dysregulation in disease

As mentioned above, dysregulation of ClpP activity by small molecules shows promise as antibacterial and anticancer agents (Bhandari et al., 2018; Wong & Houry, 2019; Ye et al., 2017). For example, ADEP4 treatment in combination with rifampicin cleared *S. aureus* biofilms in mice (Figure 1.4A) (Conlon et al., 2013). Furthermore, combinations of ADEP4 with rifampicin, linezolid, or ciprofloxacin were effective at killing stationary phase *S. aureus* cultures *in vitro* (Figure 1.4A). Conlon and colleagues suggest that ADEP targeting unique pathways might help kill these resistant populations. Additionally, there might also be crosstalk between ClpP activation and the other pathways targeted by these drugs, such as transcription and translation. In addition to bacteria, ADEPs 28 and 41 bind and activate HsClpP specifically to cause cell death (Wong et al., 2018). The structurally unique imipridones, such as ONC-201, also activate HsClpP showing

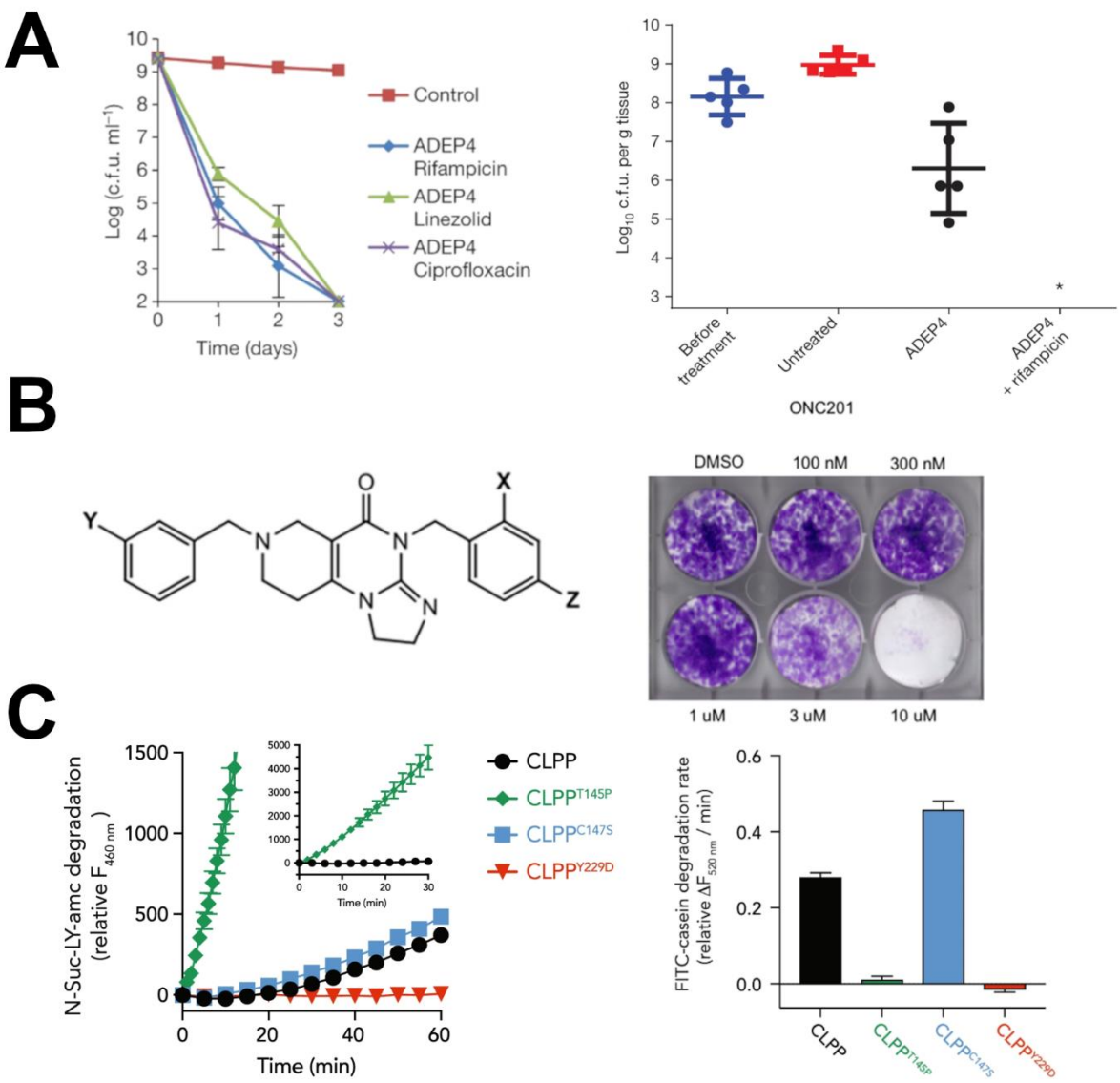

Figure 1.4 The role of ClpP in infection, cancer and Perrault syndrome. (A) (left) ADEP4 in combination with other treatments kills persisters *in vitro*. (right) ADEP4 in combination with rifampicin eradicates biofilm infection in mice. Figures adapted from (Conlon et al. 2013). (B) (left) The chemical structure of ONC201 with X, Y, and Z being CH_3, H, and H respectively. (right) Growth of SUM159 cells assessed by crystal violet staining. Figures adapted from (Graves et al. 2019). (C) (left) Peptidase activity of ClpP Perrault syndrome mutations against N-Suc-LY-amc. (right) Protease activity against FITC-Casein in the presence of HsClpX and ATP. Figures adapted from (Brodie et al. 2018).

promise against a wide range of cancers (Figure 1.4B) (Bhandari et al., 2018; Graves et al., 2019; Wong & Houry, 2019). All these compounds bind ClpP in its hydrophobic pocket and would compete for motor protein binding. Therefore, understanding the basic biology of ClpP in the absence of a motor protein might help refine the current models for how these molecules function.

ClpP activity has been shown to be important for several organisms such as *Salmonella typhimurium, L. monocytogenes, S. aureus, and S. pneumonia* (reviewed in Bhandari et al., 2018). In these cases, inhibiting ClpP activity is also effective in reducing virulence. β-lactones were among the first compounds to show promise *in vitro*, but have faced complications *in vivo* (Moreno-cinos et al., 2019). Since the β-lactones, there have been many compounds shown to inactivate ClpP by targeting its active site or affecting its oligomeric state. Interestingly, molecules that inhibit HsClpP also showed therapeutic activity against leukemia (Wong & Houry, 2019); thus, modulation of ClpP activity in either direction has the potential to affect human disease.

In humans, recessive mutations in ClpP cause Perrault Syndrome (Jenkinson et al., 2013). This disorder causes sensorineural hearing loss and ovarian disfunction in females. In one family, ClpP mutations were found within the hydrophobic pocket which would presumably affect its ability to bind the ClpX motor protein (Jenkinson et al., 2013). A future study examined two of these mutations, T145P and C147S, and showed that T145P had decreased motor binding while C147S bound similar to wild type (Brodie et al., 2018). Interestingly, these mutants were extremely different in their peptidase activities. T145P showed a dramatic increase in peptidase activity against a dipeptide substrate but not against FITC-Casein (Figure 1.4C). In contrast, the peptidase activities of C147S were slightly higher than wild type for both substrates. Furthermore, Brodie and colleagues also characterized a Perrault Syndrome mutation that occurs near the ClpP active site, Y229D. This mutation inactivated HsClpP peptidase activity and decreased ClpX binding. These data suggest that Perrault Syndrome mutations are extremely diverse and cannot be explained solely by ClpP activity or motor binding. Perhaps the mechanical properties of these mutants might better explain how their unique biochemical signatures lead to similar phenotypes. Overall, better understanding how ClpP functions in the absence and presence of AAA+ motors would potentially have implications for our understanding of Perrault Syndrome mutations.

1.9 History of single molecule studies of ClpXP and ClpAP

The ClpXP and ClpAP machines have both been well studied at the single molecule level. For more in depth reviews regarding motor proteins see (Olivares et al., 2015, 2018). For this review, I will highlight gaps of knowledge within single molecule studies that show roles where ClpP might play a role in degradation mechanics. A majority of these studies use optical trapping to apply and measure piconewton forces while observing translocation with nanometer and millisecond accuracy (Moffitt et al., 2008; Neuman & Block, 2004). From these studies we know that together, the ClpXP and ClpAP machines are highly processive enzymes (M.-E. Aubin-Tam et al., 2011; Cordova et al., 2014; Maillard et al., 2011; Sen et al., 2013) that hydrolyze ATP to unfold, translocate, and degrade protein substrate. But what does each component individually contribute to degradation mechanics, and how does their mutual activation affect these mechanics?

To begin this section, I will consider a historical perspective of single molecule data on ClpXP and ClpAP. One of the first single molecule studies of ClpXP published used total internal reflection fluorescence microscopy (TIRF) to watch ClpXP degrade a GFP substrate (Shin et al., 2009), confirming the processivity and stochastic nature of this machine. This set the stage for the same group from MIT/Vanderbilt to publish a single molecule optical tweezers analysis of ClpXP degrading a multidomain filamin substrate (M.-E. Aubin-Tam et al., 2011). They found that the machine was biochemically limited, produced around 5kT of work per step, and stalled near 33pN of force. Similar findings were published in the same year by a competing lab from UC Berkley (Maillard et al., 2011) that watched ClpXP degrade a GFP substrate. Two years later, the Berkley group reported a 1nm fundamental step size with ClpXP often taking larger bursts of steps (Sen et al., 2013). This finding was confirmed by the MIT/Vanderbilt group using various multidomain titin substrates (Cordova et al., 2014). Both labs presented models where stochastic hydrolysis by one or more ATPase subunits contributed to the bursts of motion taken by ClpXP. Following this, the MIT/Vanderbilt group showed that the pore-1 loops of ClpX are responsible for

gripping substrates during unfolding but not translocation (Iosefson, Olivares, et al., 2015). Afterwards, the Berkley group showed that both ATP hydrolysis and phosphate release occurred during the power stroke (Rodriguez-Aliaga et al., 2016). Next, the MIT/Vanderbilt group showed that the direction of degradation impacted substrate processing (Olivares et al., 2017). ClpXP unfolded titin substrates more quickly from the N terminus, but it also translocated more slowly and took smaller steps in this direction. Overall, these findings have established that force production, substrate grip, and step size are all key properties of these AAA+ proteases that govern their mechanics and function. Therefore, mechanical contributions by ClpP to any of these properties would shift the current understanding of degradation in the field and impact our understanding of their biological function as machines with two components.

1.10 Possible contributions by ClpP to previous single molecule studies

From all these studies, the prevailing model in the field is that ClpXP grips substrates with its pore-1 loops and has a fundamental 1nm step size. What remains unclear is the physical basis for the 4nm bursts of steps observed for ClpXP in single molecule experiments. Perhaps it is due to stochastic hydrolysis by several sequential motor subunits. However, this is unlikely as a mutant ClpX with only two wild type ATPase monomers still took 1-4nm steps (Cordova et al., 2014). To complicate matters, the most recent cryo-EM structures support a model in which ATP hydrolysis fuels a fundamental 1nm step for each ATPase monomer (Lopez et al., 2020; Ripstein et al., 2020). The MIT/Vanderbilt group offers a separate model from their structural data, where one ClpX monomer translocates in the opposite direction to account for the larger steps taken by ClpXP (Fei et al., 2020). Overall, more evidence is needed to conclude the physical mechanism by which ClpXP takes larger bursts of up to 4nm steps. However, it is possible that ClpP might contribute to some of the motion seen within these single molecule data. For example, the head to head distance from the extended to the compressed conformations of SaClpP differs by 12

angstroms or 1.2nm (Ye et al., 2013). Thus, concerted motion by both ClpX and ClpP may partially account for these larger bursts observed at the single molecule level. In summary, conformational changes by ClpP may contribute to ClpXP steps measured using optical tweezers by both the MIT/Vanderbilt and Berkley groups. Additionally, ClpP might also contribute to other parts of the chemomechanical cycle for both ClpXP and ClpAP.

From the earliest single molecule studies of ClpXP, the data suggest both the motor and peptidase contribute to degradation mechanics. Aubin-Tam and colleagues (M.-E. Aubin-Tam et al., 2011) watched ClpXP degrade a multidomain filamin substrate and compared translocation by ClpXP to ClpX alone. With ClpX alone they saw large backslips and other non-processive behavior that were not present in traces with ClpXP. Similarly, Maillard and colleagues (Maillard et al., 2011) confirmed these findings while studying ClpXP degrading various multidomain GFP and titin substrates. In this study, they found that ClpX alone slipped more frequently than ClpXP and that the ClpX slips were much larger in comparison. However, they noted that ClpXP had longer dwells before unfolding on average. Taken together, these two studies of ClpXP show that the ClpX motor has mechanical defects that are suppressed by ClpP binding and/or activity. One potential explanation is that ClpP provides additional substrate grip through hydrophobic contacts within its chamber. This idea is supported by single turnover studies showing that ClpXP unfolds GFP faster when it has a longer linker between GFP and the ssrA tag (Martin et al., 2008). However, it remains unclear how ClpP binding and/or activity contributes to the reduced backward slipping seen in studies of ClpX alone.

In addition to ClpX, both single molecule and solution studies of ClpA suggest that ClpP binding and/or activity affects its degradation mechanics. In solution, ClpA unfolds a dimeric protein substrate more slowly than the ClpAP complex (Baytshtok et al., 2015). Furthermore, in single turnover conditions ClpAP takes faster and longer steps than ClpA alone (Miller et al., 2013; Rajendar & Lucius, 2010). To our knowledge, no single molecule optical tweezer study has compared ClpA processing to ClpAP processing on the same substrate. From the few single

molecule studies of ClpAP performed, we know that ClpAP unfolds substrate more quickly than ClpXP but takes smaller steps and moves slower than ClpXP (Olivares et al., 2014, 2017). These differences are likely caused by the double ring architecture of ClpA, which might increase processivity and decrease stalling when processing substrate (Kotamarthi et al., 2020). Overall, both ClpA and ClpX show mechanical defects in the absence of ClpP, suggesting that ClpP binding and/or activity contributes to protein degradation mechanics by these machines.

1.11 Thesis Overview

Is mechanical contribution by ClpP unique to these enzymes or a feature of all AAA+ proteases? After all, there are many AAA+ proteases in the cell that feature similar architectures while degrading unique substrates. Recently, I published a first author paper examining the mechanical activity of ADEP-ClpP at the single molecule level using optical tweezers (Walker & Olivares, 2022). Briefly, I found that activated ClpP gripped an unfolded protein substrate against external load, withstanding up to 40pN of force and forming interactions for hundreds of seconds at low force. This work will be detailed in chapters 2 and 3.

How do my findings impact the immediate single molecule fields, and our broader understanding of ClpP biology? These questions will be addressed more fully in chapter 4. To summarize, it is possible that the peptidase components of all AAA+ proteases contribute to degradation mechanics through substrate binding. Furthermore, defining substrate grip by ADEP-ClpP has potential impacts on our understanding of substrate selection by ADEP-ClpP. Here, I provide evidence that the ClpP peptidase grips protein substrate against external load, and that the active site serine to alanine mutation had little effect on the rupture force distributions of ADEP-ClpP (Walker & Olivares, 2022). This directly impacts our understanding of previous single molecule studies of ClpAP and ClpXP. Overall, the hypothesis that the peptidase component of

AAA+ proteases contribute to mechanical degradation needs to be tested further to conclude if this is a general feature or specific to chemically activated ClpP.

CHAPTER 2

Materials and methods

2.1 Biochemical purification of ClpP and substrate proteins

Full length *E*. coli ClpP with a C-terminal hexahistidine tag and a terminal cysteine residue, and a substrate protein comprising an N-terminal HaloTag domain, four variant titin^{I27} domains (V13P), and a C-terminal hexahistidine tag and 11-amino acid ssrA degron were cloned and purified as previously described (Cordova et al., 2017). Briefly ClpP was cloned into the pQE70 plasmid and expressed in JK-10 cells, which lack endogenous ClpP (Kenniston et al., 2003). Cells were initially grown to OD_{600} ~0.6 in LB broth at 30°C, cooled to 18°C, and induced with 0.5 mM IPTG for expression overnight. Cells were harvested and resuspended in lysis buffer (50 mM sodium phosphate pH 8.0, 1 M NaCl, 5 mM imidazole, 10% glycerol), frozen in liquid nitrogen, and stored at -80°C. For purification, all the following steps were performed at 4°C unless noted otherwise. Cells were thawed and lysed with two passes through an Emulsiflex high-pressure homogenizer (Avestin, Canada). The lysate was clarified by centrifugation at 30,000 x g for 30 minutes. Clarified lysate was passed through an INDIGO-Ni (Cube Biotech, Germany) affinity column, washed, and eluted with lysis buffer containing 500 mM imidazole. Fractions were analyzed by SDS-PAGE, pooled, and concentrated to ~1 mL. Concentrated protein was further purified by size exclusion chromatography using a HiPrep 16/60 Sephacryl S300-HR column (Cytiva) equilibrated with storage buffer (50 mM Tris-HCl pH 8.0, 150 mM KCl, 0.5 mM EDTA, 10% glycerol). Fractions were analyzed by 12% SDS-PAGE and appropriate fractions pooled, concentrated using an Amicon Ultra-15 10kDa MWCO centrifugal filter (Millipore Sigma), flash frozen and stored at -80°C. ClpP was biotinylated at the terminal C-terminal cysteine using EZ-Link™ Maleimide-PEG2-Biotin (Thermo Scientific). First a 20 mM stock of the biotin-maleimide was made in storage buffer and added to a final concentration of 20x molar excess to ClpP. The

sample was left rotating at 4°C overnight and buffer exchanged into storage buffer containing 1 mM DTT before freezing with liquid nitrogen. Protein concentration was determined in storage buffer using ε_{280}=125,160 M^{-1} cm^{-1} for the ClpP tetradecamer.

The substrate protein was cloned into a pFN18A plasmid (Promega) and expressed in BL21(DE3) cells. Cells were grown to OD_{600} ~0.6 in LB broth at 37°C, cooled to 25°C, and induced with 1 mM IPTG for 3 hours. Cells were harvested by centrifugation at 4000 x g for 15 min, resuspended in lysis buffer (50 mM sodium phosphate pH 8.0, 500 mM NaCl, 10% glycerol, 10 mM β-mercaptoethanol, 20 mM imidazole) and flash frozen in liquid nitrogen for storage at -80°C. Lysis, clarification, and INDIGO-Ni affinity was performed as described above eluting with 250 mM imidazole. Fractions were analyzed by 12% SDS-PAGE. Pure fractions were pooled, concentrated, flash frozen in small aliquots. Protein concentration was determined using ε_{280}=89,380 M^{-1} cm^{-1}. For titin domain carboxymethylation, aliquots of substrate were first unfolded using 2 M guanidine-HCl at room temperature for 1.5 hours. Then, a fresh stock of 0.5 M iodoacetic acid was added to a final concentration of 2.5 mM. After another 1.5-hour incubation, the reaction was quenched by adding excess 1 M DTT to a final concentration of 10 mM. Samples were buffer exchanged into PD buffer (25 mM Hepes pH 7.6, 100 mM KCl, 10% glycerol, 10 mM $MgCl_2$, 0.1% Tween-20) and flash frozen for storage at -80°C.

2.2 Single-molecule optical trapping of ClpP-substrate complexes

For trapping experiments, biotinylated ClpP and substrate were immobilized onto 1.25-micron streptavidin beads (Spherotech) in PD buffer supplemented with 1 mg/mL BSA (PD-BSA). For substrate, we constructed a 3500 bp linker with a 3' 20 bp overhang from the M13mp18 plasmid (Bayou Biolabs) by PCR using these primers (Integrated DNA Technologies): TTTCCCGTGTCCCTCTCGA-T/idSp/TTGAAATACCGACCGTGTGA, and AATCCGCTTTGCTTCTGAC with a 5' biotin. The complement to the 20 bp overhang with

sequence ATCGAGAGGGACACGGGAAA contained a 5' phosphate and 3' amine to which a HaloTag substrate was conjugated using a HaloTag succinimidyl ester O4 ligand (Promega). The 3500 bp DNA linker was ligated in the presence of CM-titin at room temperature for >1 hour before conjugating to streptavidin beads.

All optical trapping data were collected using a dual-laser m-Trap Optical Tweezers system (LUMICKS) equipped with a 5-channel laminar flow microfluidics device. Prior to experiments, the microfluidic chip was washed extensively with ddH_2O and equilibrated with PD-BSA for >30 min. ClpP and substrate beads were washed and resuspended in PD-BSA containing an oxygen scavenging system (0.25 mg/mL glucose oxidase, 0.03 mg/mL catalase, 3 mg/mL glucose; PD-BSA-OX). ClpP-bound beads and substrate beads were flown into the 2^{nd} and 5^{th} channels, with the 3^{rd} and 4^{th} containing PD-BSA-OX and PD-BSA-OX supplemented with 10 μM ADEP1 (Cayman Chemical), respectively. Custom Python scripts were written and used to automate bead capture, force ramp/clamp control, and to perform data analysis. For rupture force experiments, after capturing beads with each trap and forming a tether, the script moved the beads at a constant velocity until a rupture occurs. Similarly, for lifetime traces the script steered the trap until a defined force is reached, after which it paused until the tether ruptures. Traces with incorrect contour lengths or multiple ruptures were discarded to avoid non-specific interactions and multiple tethers.

2.3 Optical trapping data analysis

Data analysis for both lifetime and rupture force experiments were carried out using custom Python scripts with the LUMICKS Bluelake software. For rupture force measurements, force data were first downsampled to 15 Hz using a moving mean to match distance measurements. Then, rupture forces were found by using the first derivative of the force data. For lifetimes, the end of the force ramp and the terminal rupture were both reported using the first

derivative of the force data. For lifetimes, data were downsampled further to 5 Hz, which was necessary to automate detection of the last point of the force ramp. Then, lifetimes were calculated by taking the difference between the two timepoints and the force was averaged over the duration of each lifetime.

After finding rupture forces, plotted data were fit to the Evans-Ritchie (Evans & Ritchie, 1997) and Dudko-Hummer-Szabo (Dudko et al., 2006) models for molecular adhesions to extract the intrinsic time constant and distance to transition state. Where τ is the intrinsic lifetime, r is the loading rate, $x^{\ddagger}$ is the distance to transition state, and v is a variable that represents the shape of the free energy barrier (1/2 for a cusp and 2/3 for a linear-cubic). From these fits, we also calculated the most probable rupture forces (F^{*}). We fit the distance to transition state globally for both models as it varied little with the loading rate.

$$\text{Evans-Ritchie: } P(F) = \tau^{-1} r^{-1} e^{\left\{\frac{Fx^{\ddagger}}{k_B T} - \frac{k_B T}{\tau r x^{\ddagger}}\left(e^{\frac{Fx^{\ddagger}}{k_B T}} - 1\right)\right\}}$$

$$F^{*} = \frac{K_B T}{x^{\ddagger}} \ln\left(\frac{r x^{\ddagger} \tau}{k_B T}\right)$$

$$\text{Dudko-Hummer-Szabo: } P(F) = r^{-1} * k(F) e^{\left(\frac{1}{\tau x^{\ddagger} r}\right)} e^{-\left[\frac{k(F)}{x^{\ddagger} r}\right]\left[1-\left(\frac{\nu F x^{\ddagger}}{\Delta G^{\ddagger}}\right)\right]^{1-1/\nu}}$$

$$\text{With } k(F) = \tau^{-1}\left(1 - \frac{\nu F x^{\ddagger}}{\Delta G^{\ddagger}}\right)^{\frac{1}{\nu}-1} e^{\Delta G^{\ddagger}\left[1-\left(1-\frac{\nu F x^{\ddagger}}{\Delta G^{\ddagger}}\right)^{\frac{1}{\nu}}\right]}$$

2.4 Biochemical degradation assays

FITC-Casein (Pierce™ Fluorescent Protease Assay Kit, Thermo Scientific) was prepared as directed to 5 mg/mL in ddH_2O and stored at -20°C. For experiments, reactions were made in PD buffer without FITC-Casein and incubated at 30°C for >10 minutes. After incubation, FITC-Casein was added to final concentration of 0.1 mg/mL and 50 μL reactions were pipetted into a 384 well plate (Greiner Bio-One). The fluorescence was tracked using a Biotek Syngergy HTX multi-mode plate reader (Agilent Technologies) every 30 seconds with excitation/emission

wavelengths of 502/528 nm. Similarly, for CM-titin degradation, reactions were made in PD buffer without substrate and incubated at 30°C for >10 minutes, after which CM-titin was added to a final concentration of 2 μM and time started. Each time point taken was quenched with a final concentration of 2x SDS-PAGE assay buffer and flash frozen in liquid nitrogen. Samples were boiled at 95°C for 5 minutes and 12% SDS-PAGE followed by staining with Coomassie Brilliant Blue.

CHAPTER 3

The activated ClpP peptidase forcefully grips a protein substrate

This chapter was published in its entirety in Biophysical Journal (Walker & Olivares, 2022). I performed all experiments and data analysis under the direction of Dr. Adrian Olivares. The manuscript was prepared by both of us, with input and revisions from my labmate Dr. Jennifer Norton and colleagues Dr. Matthew Lang and Dr. Marija Zanic. Chapter 2 details the materials and methods used in this paper and were also published in the same article in Biophysical Journal. I have included the supplemental figures within the text of this chapter.

3.1 Abstract and statement of significance

ATPases Associated with diverse cellular Activities (AAA+) proteases power the maintenance of protein homeostasis by coupling ATP hydrolysis to mechanical protein unfolding, translocation, and ultimately degradation. Though ATPase activity drives a large portion of the mechanical work these molecular machines perform, how the peptidase contributes to the forceful denaturation and processive threading of substrates remains unknown. Here, using single-molecule optical trapping, we examine the mechanical activity of the Caseinolytic Peptidase P (ClpP) from *Escherichia coli* in the absence of a partner ATPase and in the presence of an activating small molecule acyldepsipeptide. We demonstrate that ClpP grips protein substrate under mechanical loads exceeding 40 pN, which are greater than those observed for the AAA+ unfoldase ClpX and the AAA+ protease complexes ClpXP and ClpAP. We further characterize substrate-ClpP bond lifetimes and rupture forces under varying loads. We find that the resulting slip bond behavior does not depend on ClpP peptidase activity. Additionally, we find that unloaded bond lifetimes between ClpP and protein substrate are on a timescale relevant to unfolding times

(up to ~160 s) for difficult to unfold model substrate proteins. These direct measurements of the substrate-peptidase bond under load define key properties required by AAA+ proteases to mechanically unfold and degrade protein substrates.

Energy-dependent proteases drive essential protein degradation to maintain cellular homeostasis and to rapidly regulate protein levels in response to changes in cellular environment. Using single-molecule optical tweezers, several studies demonstrate that the molecular process of degradation involves the mechanical unfolding and translocation of protein substrates by the ATP hydrolyzing enzyme component of these protease complexes. This study provides evidence that the chambered peptidase component of these molecular machines also contributes to the mechanical process of degradation by gripping substrate under load in a manner independent of peptide hydrolysis. Our results suggest that the peptidase actively contributes to the biophysical mechanisms underlying processive protein degradation by energy-dependent proteolytic machines.

3.2 The role of ClpP as a AAA+ peptidase

AAA+ (ATPases Associated with diverse cellular Activities) proteases power protein degradation in the cell to eliminate damaged or misfolded proteins and control cellular processes by modulating protein levels. These proteolytic molecular machines comprise ATP-dependent, ring-shaped motor proteins (i.e. AAA+ protein unfoldases) that recognize, unfold and translocate substrate protein into a self-compartmentalized peptidase (Olivares et al., 2015, 2018). In *Escherichia coli*, the ClpP peptidase pairs with the AAA+ unfoldases ClpA and ClpX to form functional AAA+ proteases (Burton et al., 2001; Maurizi, Clark, Kim, et al., 1990). Importantly, protein degradation is processive (i.e., enzyme translocates along protein substrate without dissociating until degradation is complete). Robust processivity requires that the probability of substrate dissociation is low and that subunits within the translocating machinery maintain

enzymatic cycles out of phase such that polypeptide does not dissociate during substrate unfolding and translocation.

Single-molecule studies in the past decade have illuminated how the AAA+ proteases ClpXP and ClpAP function during processive protein unfolding and translocation. More specifically, optical trapping experiments combined with solution biochemistry revealed how AAA+ proteases generate force, coordinate ATPase cycles, grip protein substrate, and translocate along the polypeptide track (M.-E. Aubin-Tam et al., 2011; Cordova et al., 2014; Iosefson, Olivares, et al., 2015; Kotamarthi et al., 2020; Maillard et al., 2011; Olivares et al., 2014, 2017; Rodriguez-Aliaga et al., 2016; Sen et al., 2013). Because the AAA+ unfoldase behaves as a motor protein (i.e., couples chemical energy in the form of ATP hydrolysis to physical translocation along a macromolecular track) and unfolds and translocates substrate protein in the absence of its proteolytic partner, the peptidase has been overlooked as contributing to the chemomechanical cycle of protein degradation by AAA+ proteases. In fact, there is little direct evidence that ClpP generates force during the process of protein degradation. However, the AAA+ motors show mechanical defects when ClpP is not present. For example, ClpA unfolds a dimeric substrate more slowly (Baytshtok et al., 2015) and takes slower kinetic steps in the absence of ClpP (Miller et al., 2013; Rajendar & Lucius, 2010). Moreover, ClpX, which grips substrate via its pore-1 loops (Iosefson, Nager, et al., 2015; Iosefson, Olivares, et al., 2015; Rodriguez-Aliaga et al., 2016), slips on substrate more often than ClpXP (Iosefson, Olivares, et al., 2015). Though differences in motor function can be partially explained by changes in ATPase activity in the presence of ClpP (Hinnerwisch et al., 2005; Kim et al., 2001), we sought to test if ClpP participates mechanically during protein degradation since direct observation of ClpP mechanics has not been demonstrated. Additionally, another group used atomic force microscopy to characterize the mechanics of the architecturally similar proteasomal 20S core particle engaging a model protein substrate in the absence of a AAA+ partner. The study concluded that the 20S active site

threonine significantly contributes to observed high force rupture events measured between peptidase and substrate (Classen et al., 2011).

3.3 ADEPs activate ClpP for proteolysis

Obtaining direct evidence of ClpP mechanical degradation has been complicated as ClpP poorly degrades large unfolded protein substrates in the absence of AAA+ motors due to gating by its N-terminal loops (Gribun et al., 2005; Jennings et al., 2008). AAA+ unfoldase binding activates ClpP by opening the axial pore and allowing polypeptide to be threaded into the ClpP chamber for degradation. However, a class of natural products called acyldepsipeptides (ADEPs) activate ClpP in the absence of motor proteins (Brötz-Oesterhelt et al., 2005; Malik & Brötz-

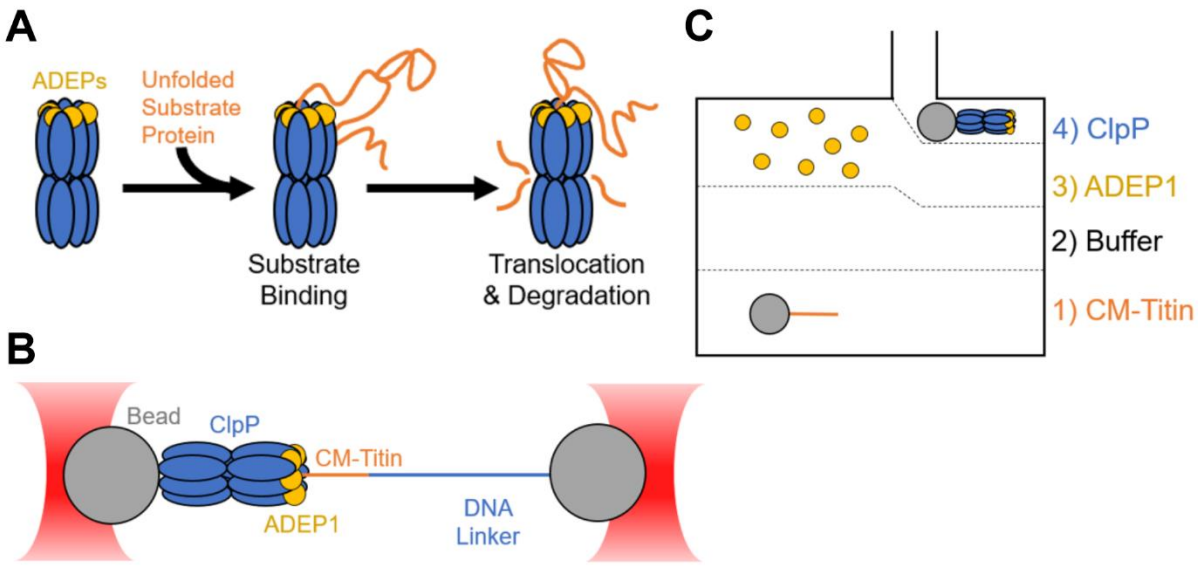

Figure 3.1 Measuring single-molecule ClpP mechanics by optical trapping. (A) Cartoon of ADEP1 activation of ClpP. ADEP1 (yellow) binds to the ClpP tetradecamer (blue), opening its central pore and allowing metastable protein substrates (orange) to enter and be degraded. (B) Schematic of optical trapping assays. ClpP is immobilized to one laser-trapped bead and engages a CM-titin substrate bound to a different bead using a 3500bp DNA linker. (C) Example schematic of the flow cell used for optical trapping showing a top-down view. Solutions were prepared separately and flown into the channels as shown. Single substrate- and ClpP-coated beads were captured in channels 1 and 4, respectively. The stage was then moved to channel 3 where experiments were performed in the presence of 10 μM ADEP1.

Oesterhelt, 2017), allowing the direct observation of protein degradation by ClpP (Fig. 3.1 A). ADEPs bind to the same hydrophobic pocket on ClpP that motors bind (Amor et al., 2016) and are thought to activate ClpP in a similar manner, i.e. by causing rearrangement of the ClpP N-terminal loops (Gersch et al., 2015). In cells, this activation leads to indiscriminate proteolysis and ultimately cell death, making ClpP a promising target for developing antibiotics that hamper pathogenic biofilm formation (Conlon et al., 2013) and anti-cancer therapies due to ClpP's conserved role in mitochondrial protein homeostasis (Graves et al., 2019; Moreno-cinos et al., 2019). Additionally, ADEPs disrupt bacterial cell division through the specific degradation of the protein FtsZ by ClpP (Sass et al., 2011). Furthermore, using purified proteins, ADEP-activated ClpP appears to unfold and degrade FtsZ *in vitro* without the need for motor proteins (Silber et al., 2020). Taken together, these data suggest that ClpP is capable of mechanically engaging and degrading substrate in the absence of a AAA+ unfoldase.

Here, we aim to provide evidence of ClpP's contribution to mechanical protein degradation in the absence of motor proteins. We hypothesize that ClpP grips and degrades substrate against external force, and that the active site serine contributes to substrate grip. Using single-molecule optical trapping, we do not observe denatured substrate translocation but demonstrate that ClpP grips substrate against applied loads in excess of 40 pN when activated by ADEP1. We find that substrate-ClpP bond lifetimes and rupture forces decrease as external load increases consistent with slip bond behavior. We further show that active site inactivation does not significantly affect substrate grip and discuss what other portions of ClpP likely account for its mechanical behavior. To our knowledge, this study provides the first direct evidence that ClpP maintains a force-dependent grip on protein substrates without a motor protein and suggests additional activities that ClpP may contribute to ATP-dependent processive translocation and protein degradation outside of its peptidase activity.

3.4 Single-molecule mechanics of the ClpP peptidase

To probe the single-molecule mechanics of ClpP engaging an unfolded protein substrate, we used a dual-laser optical trap in passive mode (Figs. 3.1 B and C) without force feedback to maintain constant force (Bustamante et al., 2021). We immobilized biotinylated ClpP to one streptavidin-coated bead and a model multidomain substrate to separate streptavidin-coated beads. The substrate comprised a HaloTag domain at its N-terminus, which was conjugated to a biotinylated 3500bp DNA linker, tandem repeats of a variant of the I27 domain of human titin (titin^{I27}) that were chemically denatured by carboxymethylating buried cysteine residues (CM-titin), and a C-terminal ssrA degron tag. For optical trapping experiments, we used a microfluidic device to introduce ClpP and substrate beads into a flow cell for staged assembly in laminar flow of the ClpP-substrate complex in the absence and presence of saturating concentrations of ADEP1 (Fig. 3.1 C). Since tethers rarely formed in the absence of ADEP1, ADEP1 was present in all optical trapping experiments. We use ADEP1 here under the reasonable assumption that ADEP binding faithfully mimics how AAA+ motors influence ClpP behavior as recent cryo-electron microscopy studies of ClpXP and ClpAP reveal nearly superimposable ClpP structures when bound to ADEPs or motors (Fei et al., 2020; Lopez et al., 2020; Ripstein et al., 2020).

First, we measured the lifetimes of the interaction between ClpP and substrate at constant force at various applied loads (Fig. 3.2 A). The interactions between ClpP and substrate were extremely stable and did not show any translocation during the experimental time course, up to 200-300 seconds. The distribution of lifetimes as a function of applied load followed a slip bond behavior and fit to the Bell model of force-dependent bond rupture between two molecules separated by a potential barrier (Bell, 1978) (Fig. 3.2 B). Specifically, we were interested in measuring the unloaded lifetime (τ_0=1/k) and the distance to the transition state ($x^{‡}$). From this fit, we obtained an unloaded lifetime (τ_0) of 158 ± 39 s and a distance to the transition state ($x^{‡}$) of 0.3 ± 0.1 nm (Mean ± SEM, N=43). We note that this unloaded lifetime is much longer than the

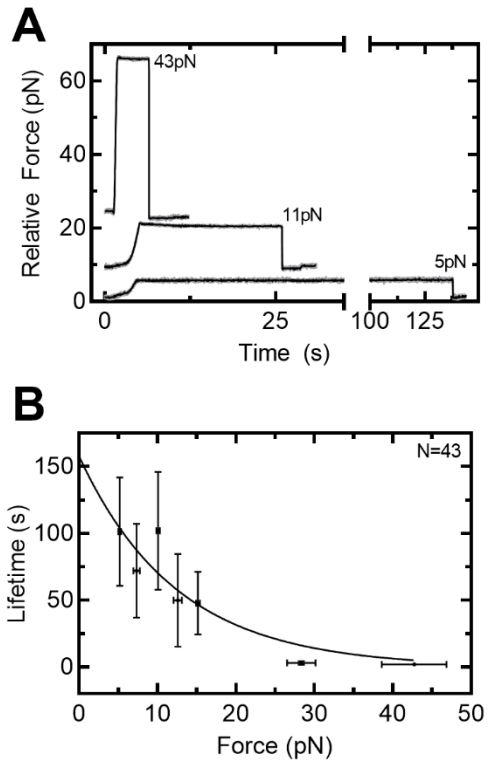

Figure 3.2 ADEP1-ClpP forms long lived interactions with protein substrate under load. (A) Example time course of ClpP interaction with CM-titin as a function of applied load. Data were downsampled to 700 Hz (gray) and 50 Hz (black). A constant speed force ramp was applied until the target force reached, after which the trap position remained constant until tether rupture back to 0 pN. (B) Tether lifetimes as a function of applied load showing the mean ± SEM in both x and y (N=8, 4, 8, 2, 9, 3 for each force from low to high). The solid line is the fit to the Bell-Evans model for a slip bond (see Methods) yielding τ_0 = 158 ± 39 s and $x^{\ddagger}$ = 0.3 ± 0.1 nm (fit ± SEM).

unfolding time constants of several substrate domains from single-molecule studies of ClpAP and ClpXP, which vary between 0.3-55 s for several variants of titin^{I27}, 0.03-3.4 s for filamin domains, and 9.1-19 s for GFP (M.-E. Aubin-Tam et al., 2011; Cordova et al., 2014; Iosefson, Nager, et al., 2015; Maillard et al., 2011; Olivares et al., 2017; Sen et al., 2013; Shin et al., 2009). The ability of ADEP-ClpP to grip substrate on timescales relevant for degradation suggests that ClpP could contribute to degradation by gripping substrates within the ClpAP/XP complexes thus preventing the substrate backslipping observed with the AAA+ motor in the absence of ClpP (M.-E. Aubin-Tam et al., 2011; Maillard et al., 2011) or premature dissociation.

Because of the observed long timescales of the experiments above and lack of translocation, we also measured rupture force as a function of loading rate to probe the mechanical strength of the interaction between ClpP and substrate. A linear force ramp was applied to the ClpP-substrate tether until a terminal rupture occurred (Fig. 3.3 A). We observed a bimodal behavior in ClpP-substrate interactions as demonstrated from the distributions of rupture forces under different loading rates (Fig. 3.3 B). To exclude the possibility of artifacts arising from tethering our enzyme-substrate complex via a DNA linker or from the experimental dual bead geometry, we examined the force-induced rupture of an oligo annealed to DNA to ensure the validity of our dual-bead assay. Our results using the same 3500bp DNA linker with a 20bp overhang with ligation were infrequent and occurred at forces different than ClpP-substrate tethers. Furthermore, the ruptures without ligation agreed with previously published literature on DNA shearing (Lang et al., 2004) and yielded different rupture forces than any of the rupture peaks observed for ClpP-substrate tethers, giving us confidence in our experimental design (Fig. 3.4).

For ClpP-substrate interactions, the rupture force distributions at different loading rates were fit to several models of bond rupture based on Kramer's Theory, the Evans-Ritchie (Evans & Ritchie, 1997) and Dudko-Hummer-Szabo (Dudko et al., 2006) models (Fig 3.3 C). From these fits, we obtained the thermal off rate (*k*), distance to the transition state ($x^{\ddagger}$), and the free energy of activation ($\Delta G^{\ddagger}$) for the ClpP-substrate complex in the presence of ADEP1 (Table 3.1). For the Evans Ritchie model, the fits for the unloaded lifetimes (τ_0=1/k) varied between 1-10 s depending on the loading rate, though this variability may represent the crossing of an energy barrier as seen for other molecular interactions (Merkel et al., 1999; Neuert et al., 2006). The Dudko-Hummer-Szabo model takes the shape of the transition state surface into account, which can be either a cusp (v=1/2) or linear-cubic (v=2/3). The (τ_0) of these fits were similar to the Evans Ritchie parameters while the ($x^{\ddagger}$) was similar for the linear-cubic and slightly larger for the cusp profile,

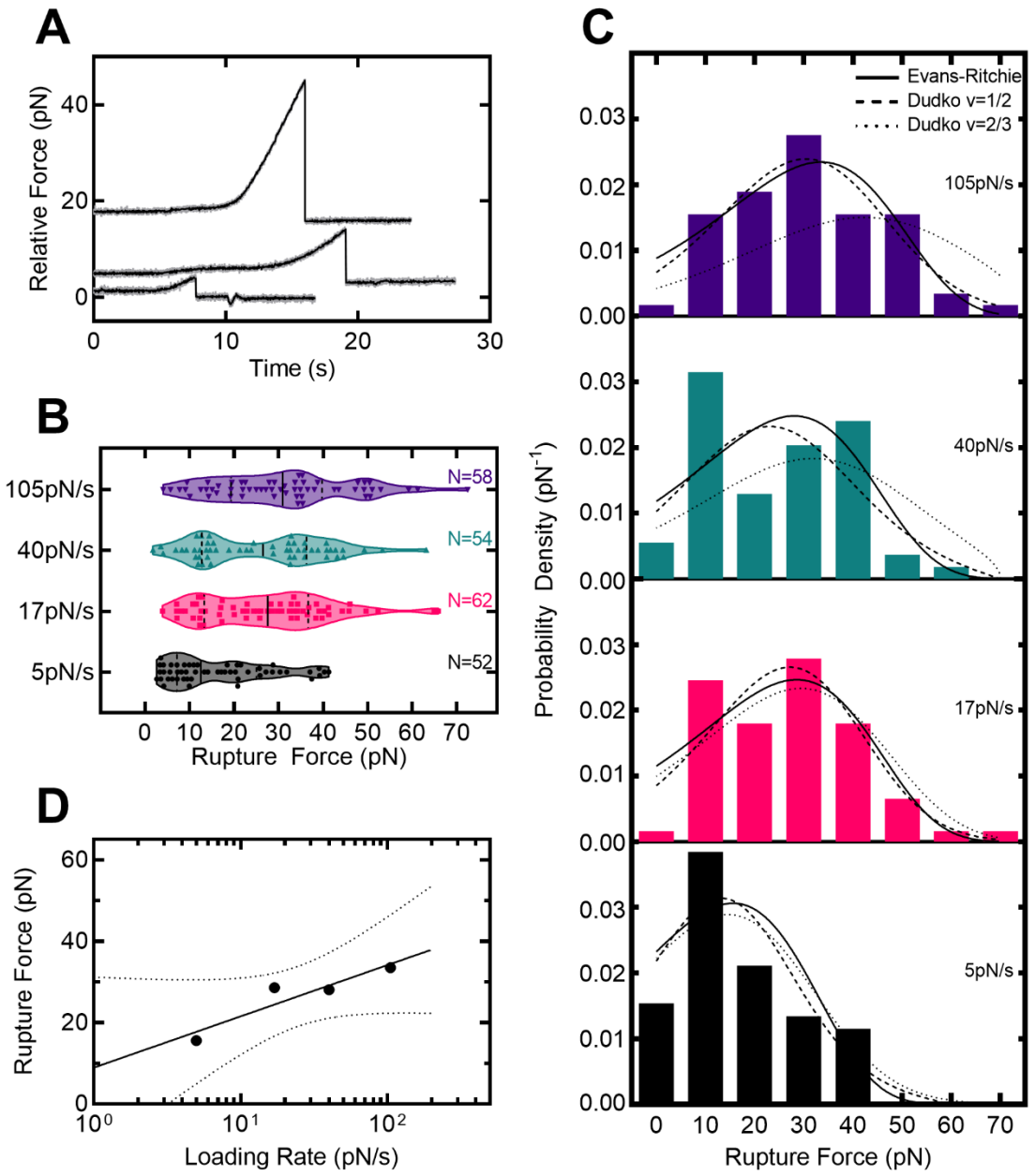

Figure 3.3 ADEP1-ClpP grips substrate against external load. (A) Example rupture force traces of ADEP1-ClpP engaging CM-titin. Data were downsampled to 700 Hz (gray) and 50 Hz (black). Example traces are offset on the y-axis for clarity. A constant speed force ramp is applied until the interaction ruptures to 0 pN. (B) Violin plots of ClpP-substrate rupture forces in the presence of ADEP1 are shown at indicated loading rates. Data points represent unique tethers with a terminal rupture to 0 pN. Vertical lines mark the median and quartiles of each distribution and N of each loading rate is shown. (C) Histograms of the rupture forces shown in (B). Fits to the Evans-Ritchie model (Evans & Ritchie, 1997) for each loading rate are shown as solid black lines along with fits to the Dudko-hummer-Szabo model (Dudko et al., 2006) where v=1/2 (dashed lines) and v=2/3 (dotted lines). (D) Most probable rupture force is plotted as a function of loading rate for wild type ClpP-substrate interactions in the presence of ADEP1.

(Continued) The most probable rupture forces shown are derived from fits of data in *(C)* to the Evans-Ritchie model. The data were fit to a semi log line with parameters b = 7.6 ± 7.3 pN and m = 13.4 ± 4.9 (Fit +/- SEM).

0.3 ± 0.1 nm and 0.4 ± 0.1 nm, respectively (mean ± SEM). The free energy of activation varied with the loading rate yielding values between 3-5 k_BT (Table 3.1). Finally, we fit the most probable rupture forces calculated from the Evans Ritchie model as a function of loading rate to a semi-log line with intercept (b) = 8.9 ± 5.2 pN and slope (m) = 12.6 ± 3.5 (Fig 3.3 D). This slope represents the force sensitivity of the interaction as it is the force necessary to increase the dissociation rate k_{off} by *e*-fold.

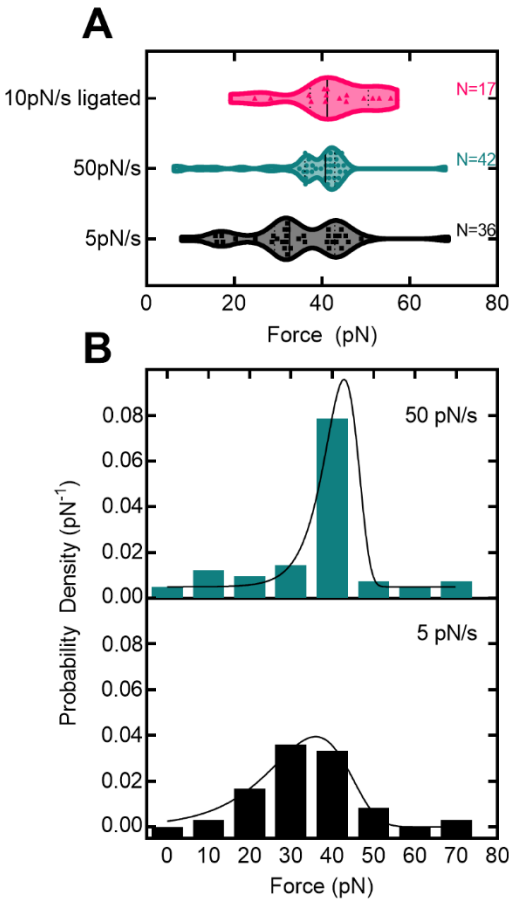

Figure 3.4 Controlling for DNA overhang effects on observed rupture forces. (A) Violin plots of observed rupture forces for control linker DNA with overhang at two different loading rates (see Methods). Data points represent unique tethers with a terminal rupture to 0 pN. Vertical lines mark the median and quartiles of each distribution. (B) Histograms of the rupture forces shown in (A). Fits to the Evans-Ritchie model for each loading rate are shown as solid black lines.

	Evans-Ritchie		Dudko-Hummer-Szabo					
			v = 1/2			V = 2/3		
Loading Rate (pN/s)	t (s)	$x^{\ddagger}$ (nm)	t (s)	$x^{\ddagger}$ (nm)	ΔG (kT)	t (s)	$x^{\ddagger}$ (nm)	ΔG (kT)
ClpPwt								
5	8.59 ± 1.44	0.22± 0.03	9.16 ± 1.90	0.37 ± 0.07	2.74 ± 0.57	8.97 ± 2.26	0.25 ± 0.07	2.93 ± 3.39
17	5.10 ± 1.16		6.88 ± 2.06		4.73 ± 2.13	5.89 ± 2.17		4.95 ± 7.33
40	2.11 ± 0.47		2.43 ± 0.77		3.19 ± 0.71	3.22 ± 1.56		2.93 ± 0.82
105	1.08 ± 0.27		1.42 ± 0.48		4.43 ± 1.59	2.24 ± 1.43		3.18 ± 0.86
ClpPS97A								
5	9.68 ± 2.11	0.25 ± 0.04	10.49 ± 3.04	0.41 ± 0.10	3.19 ± 1.13	9.34 ± 2.91	0.26 ± 0.07	4.06 ± 8.33
17	6.60 ± 1.99		9.67 ± 4.27		5.47 ± 3.06	7.48 ± 4.33		Unstable
40	2.90 ± 0.88		3.41 ± 1.66		3.19 ± 0.95	3.92 ± 2.34		2.96 ± 0.74
105	1.22 ± 0.38		1.56 ± 0.72		4.29 ± 1.67	2.78 ± 2.14		3.10 ± 0.81

Table 3.1 Fits for rupture force distributions shown in Figures 3.3 and 3.6. Table of fit parameters to the Evans-Ritchie and Dudko-Hummer-Szabo models (see Methods). Values shown are the best fit ± SEM.

3.5 Contribution of the ClpP active site serine to substrate grip

Having observed the ability of ClpP to grip protein substrate under load, we asked if we could determine what domain of ClpP contributes to the peptidase's mechanical behavior. We hypothesized that the ClpP active site serine might affect substrate grip through formation of a covalent intermediate, as observed for all serine proteases, by coordinating substrate binding, or through a combination of both mechanisms. Therefore, we first mutated the active site serine to alanine (ClpPS97A) to assess how the active site affects substrate grip. ClpPS97A inactivation was verified by monitoring the degradation of a fluorescently-labeled unfolded substrate (FITC-Casein) and of our model CM-titin substrate (Fig. 3.5). In rupture force experiments, the shape of ClpPS97A distributions remained similar to wild type ClpP (Fig. 3.6 A). We fit the distribution of

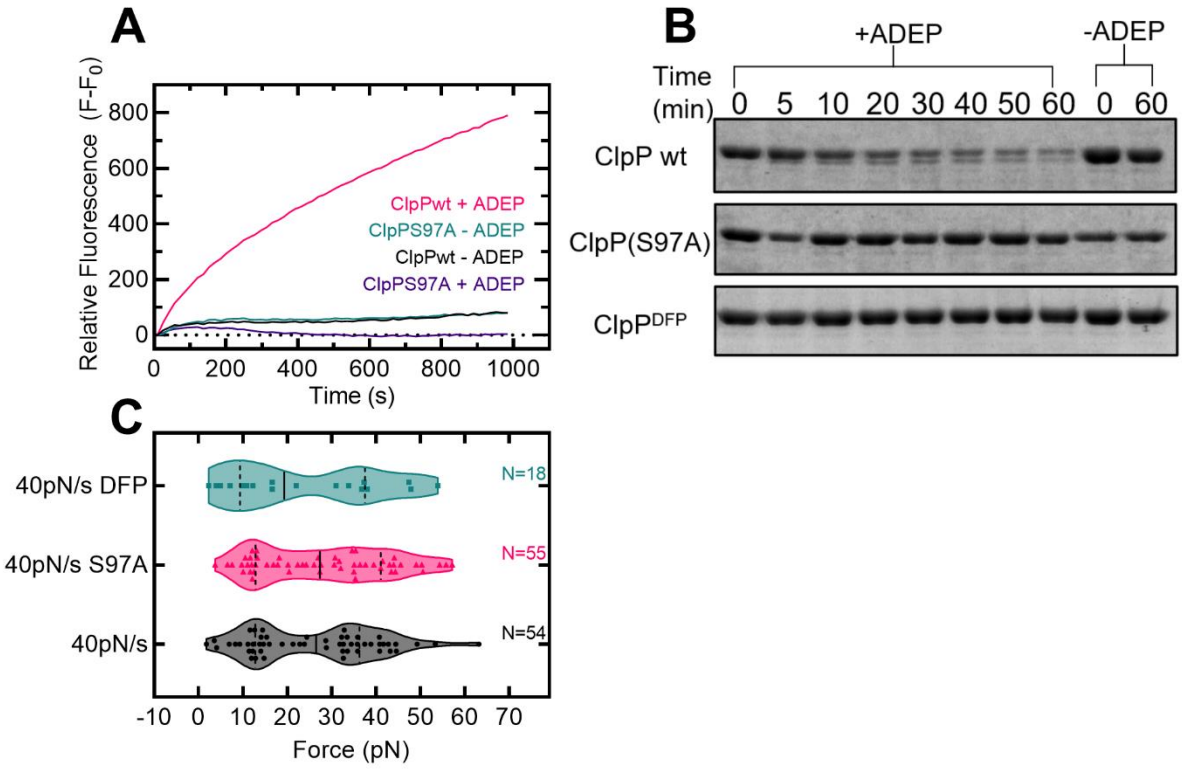

Figure 3.5 Mutation of Ser97 to Ala and DFP inactivate ClpP for degradation. (A) FITC-Casein degradation assay measuring proteolysis by ClpP. As FITC-Casein is degraded, FITC fluorescence increases over time. Only wild type ClpP is active for degradation in the presence of ADEP1 over this time course (N=1). (B) Degradation of the multidomain CM-titin substrate monitored by SDS-PAGE. ClpPS97A and DFP-ClpP do not easily degrade this substrate in comparison to wild type ClpP. C) Violin plots of rupture forces comparing wild type ClpP, ClpPS97A, and DFP-ClpP at 40 pN/s loading rate. The median and quartiles are represented by the solid and dashed lines, respectively.

rupture forces to the Evans-Ritchie and Dudko-Hummer-Szabo models, which yielded similar off rates, distance to the transition state, and free energy of activation as wild type ClpP (Fig. 3.6 B and Table 3.1). Finally, we fit the most probable rupture forces as a function of loading rate for ClpPS97A and found that the slope and intercept also remained similar to wild type ClpP. These data suggest that the ClpP active site serine does not contribute to substrate grip. In addition to the active site mutation, we used diisopropylfluorophosphate (DFP) to verify if the ClpP active site serine

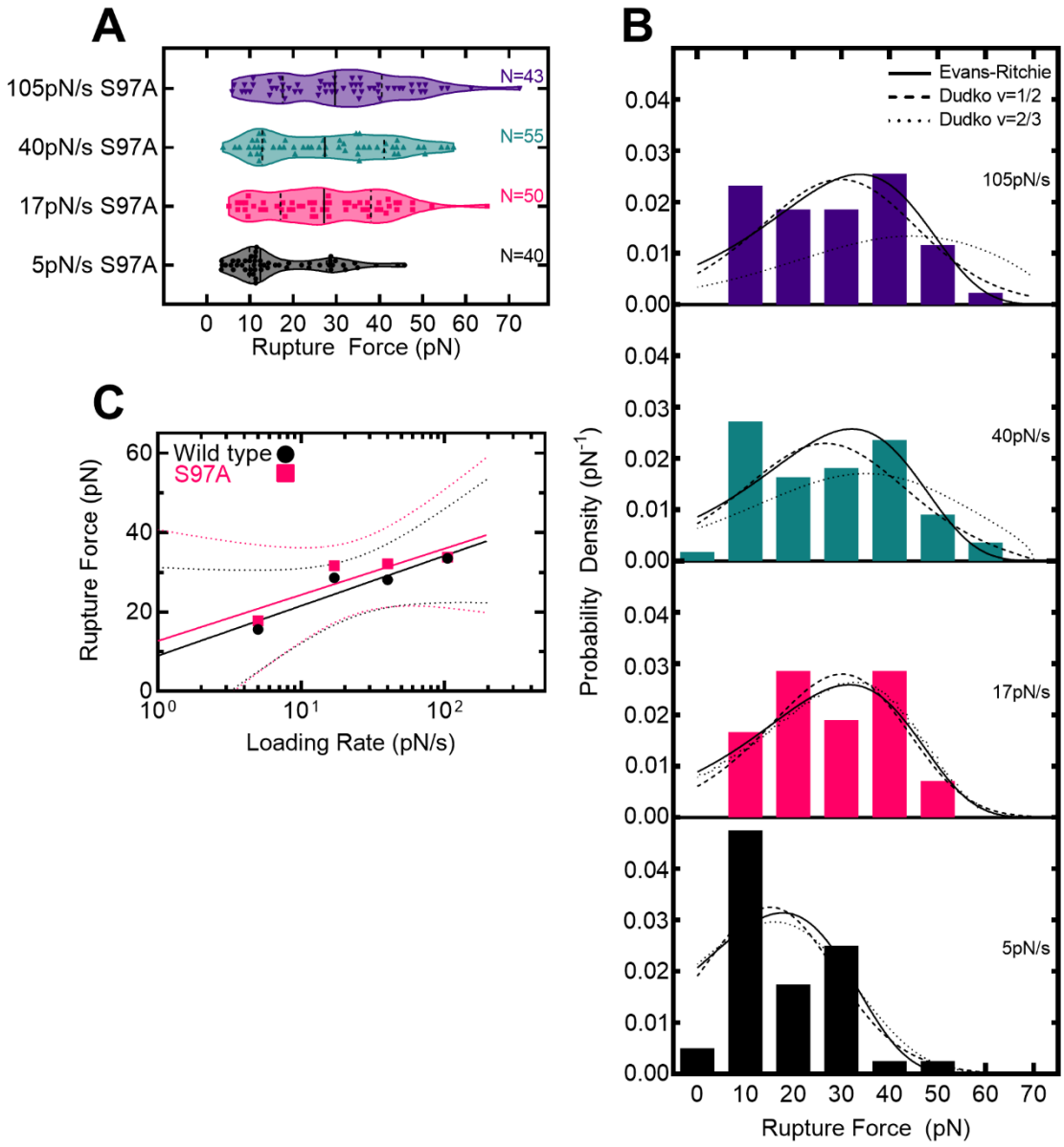

Figure 3.6 ClpP active site inactivation does not affect substrate grip. (A) Violin plots of ClpPS97A-substrate rupture forces in the presence of ADEP1 are shown at indicated loading rates. Data points represent unique tethers with a terminal rupture to 0 pN. Vertical lines mark the median and quartiles of each distribution. (B) Histograms of the rupture forces shown in (A). Fits to the Evans-Ritchie model for each loading rate are shown as solid black lines while Dudko-Hummer-Szabo fits with v=1/2 (dashed lines) and v=2/3 (dotted lines). (C) Most probable rupture force is plotted as a function of loading rate for wild type ClpP- and ClpPS97A-substrate interactions in the presence of ADEP1. The most probable rupture forces are derived from fits of data in (B) to the Evans-Ritchie model. For ClpPS97A, the data was fit to a semi log line with parameters b= 13.9 ± 6.4 pN and m = 10.5 +/- 4.3 (Fit +/- SEM).

contributes to grip, as DFP chemically inactivates ClpP. We found that the shape of the distribution still remained similar to both wild type ClpP and ClpPS97A at the tested loading rate (Fig. 3.5C). This further supports the conclusion that the ClpP active site serine is not coupled to mechanical gripping of protein substrate. Using the parameters from the Dudko-Hummer-Szabo model, we recreated the transition state energy landscapes of the observed ClpP-substrate interactions with energy wells represented as harmonic potentials (Fig. 3.7). We compared these to other measured protein-protein interactions (M. E. Aubin-Tam et al., 2011) and found that the free energy of activation and distance to the transition state are comparable to the interaction between fluorescein and an anti-fluorescein antibody. Interestingly, the transition state distance is also similar (~0.7-1 nm) to those observed for force-dependent ClpXP translocation along substrate polypeptide (M.-E. Aubin-Tam et al., 2011; Rodriguez-Aliaga et al., 2016).

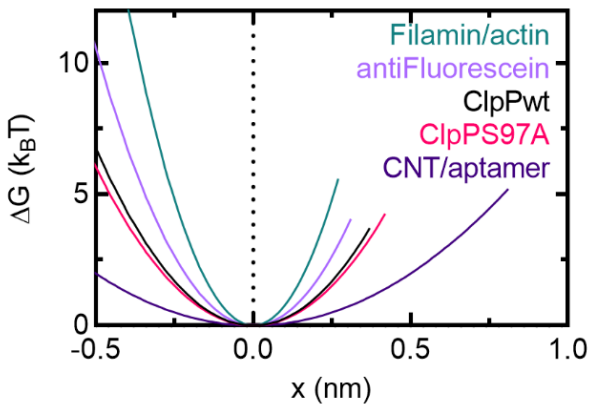

Figure 3.7 Free energy diagram of the ClpP-substrate interactions. Free energy diagrams were constructed according to the Dudko-Hummer-Szabo model (Dudko et al., 2006) assuming a cusp shape (v=1/2). Each curve represents a different interaction graphed in x until the distance to the transition state, at which point the curve stops. Both wild type ClpP and ClpPS97A show a similar energy barrier to antifluorescein-fluorescein. Values for several other interactions were taken from Refs. (Aubin-Tam et al, 2011; Lee et al., 2009) for comparison.

3.6 The impact of ClpP grip on degradation mechanics

Protein degradation by AAA+ proteases is an essential cellular process that requires the coordination of ATP-dependent motor proteins with their peptidase components. Based on single-molecule studies (M.-E. Aubin-Tam et al., 2011; Cordova et al., 2014; Iosefson, Olivares, et al., 2015; Maillard et al., 2011; Olivares et al., 2015, 2018; Rodriguez-Aliaga et al., 2016; Sen et al., 2013), the AAA+ proteases ClpXP and ClpAP produce pN forces to unfold and translocate protein substrates. The motors grip substrate using distinct pore loops (Iosefson, Nager, et al., 2015; Iosefson, Olivares, et al., 2015; Rodriguez-Aliaga et al., 2016) and drive polypeptide translocation through conformational changes between motor subunits (Cordova et al., 2014; Sen et al., 2013; Stinson et al., 2015). However, whether the peptidase, ClpP, aids mechanically to this reaction remained a question of interest. Here, using single-molecule optical trapping, we show the first evidence that ClpP grips an unfolded protein substrate against significant external load, in the absence of a AAA+ motor. The force-dependent lifetimes follow characteristic slip bond behavior (Fig. 3.2), with an average unloaded lifetime of 157 seconds. Notably, this is similar to ClpAP and ClpXP-mediated unfolding lifetimes of difficult-to-unfold substrates like the wild type titin^{I27} domain (M.-E. Aubin-Tam et al., 2011; Cordova et al., 2014; Iosefson, Nager, et al., 2015; Iosefson, Olivares, et al., 2015; Maillard et al., 2011; Olivares et al., 2017; Sen et al., 2013; Shin et al., 2009) and helps explain the trapping of substrates by proteolytically inactive ClpP variants in proteomic studies (Feng et al., 2013; Flynn et al., 2003; Neher et al., 2006). We hypothesize that the observed force-dependent interaction between ClpP and substrate contributes to overall substrate grip during AAA+ protease degradation and likely aids in preventing slipping of protein substrates. Our hypothesis is consistent with experimental data demonstrating that addition of an unfolded region prior to the folded domain of GFP-ssrA increases the unfolding and degradation speed by ClpXP (Martin et al., 2008), that slipping events are readily observed during unfolding and translocation of substrate by ClpX in the absence of ClpP (M.-E. Aubin-Tam et al., 2011; Iosefson, Olivares, et al., 2015; Maillard et al., 2011), and that a longer unstructured substrate tail

capable of reaching into ClpP compensates for reduced substrate grip by pore 1-loop variants of ClpXP (Iosefson, Olivares, et al., 2015).

Furthermore, we characterized ClpP-substrate rupture forces and fit them to models of force-dependent protein-ligand interaction based on Kramers theory (Dudko et al., 2006; Evans & Ritchie, 1997). The fits yield small distances to the transition state, ($x^{\ddagger}$=0.2-0.3nm) while unloaded bond lifetimes ($\tau=1/k_0$) vary between 1-10s depending on the loading rate (Fig. 3.3, Table 3.1). Based on these parameters, we obtain a free energy of ClpP-substrate interaction, $\Delta G \approx 4\ k_BT$, which is similar to estimates of work (~5 k_BT) produced by ClpXP and ClpAP during a power stroke (M.-E. Aubin-Tam et al., 2011; Olivares et al., 2017). Therefore, the energetics contributing to substrate grip by ClpP could provide a partial failsafe for the AAA+ protease to remain bound to a difficult to unfold substrate or under conditions of limiting ATP concentration, such as during stationary phase in bacteria (Peterson et al., 2012). During these periods of slow growth due to unfavorable conditions such as nutrient limitation, proteins could evade degradation by refolding and releasing before the motor has a chance to unfold and translocate (Nager et al., 2011).

3.7 Hypotheses for bimodal rupture force distributions

Interestingly, we find that rupture forces distribute in a bimodal fashion. Several hypotheses account for bimodality. First, at least two populations arise from interactions of the substrate with distinct ClpP conformers, such as those observed in structural studies (Kang et al., 2004; Kimber et al., 2010; Sprangers et al., 2005; Ye et al., 2013; Zhang et al., 2011). Second, ClpP possesses two substrate binding regions or sites, each responding to external force differently. We conjectured that one site would be the active site since the protease reaction proceeds through a covalent intermediate (Fig. 3.6). Here we show that mutating the active site serine to alanine did not significantly affect substrate grip by ClpP. Third, the N-terminal loops of

ClpP present another candidate site mediating substrate grip, as they already play a role in substrate gating (Gribun et al., 2005) and modulate the activity of the active site serine (Jennings et al., 2008). Likewise, different populations could arise due to a combination of multiple ClpP subunits engaging the substrate. Finally, the bimodality could be caused by the substrate's conformation as it enters the chamber of ClpP. For example, unfolded CM-titin possibly enters as or forms partially folded intermediates within ClpP that require greater force to rupture. Such structures are capable of being degraded by ClpXP as previous studies show that two polypeptide chains linked by a disulfide bond (Burton et al., 2001) and knotted protein substrates are degraded by ClpXP (Martín et al., 2017; Sivertsson et al., 2019; Sriramoju et al., 2018). Ultimately, ClpP grips protein substrate in the absence of a AAA+ motor protein, although the molecular details defining ClpP grip require further study.

Substrate grip exhibited by ClpP might have important implications for ClpAP and ClpXP. For example, ClpA's unfolding speed increases when in complex with ClpP in a manner not fully accounted for by ClpA's ATPase activation when ClpP is present, i.e. 7-fold unfolding speed increase yet 2-fold ATPase increase with ClpP (Baytshtok et al., 2015). Additionally, a ClpX variant with unfolding defects is rescued when in complex with wild type ClpP, ClpPS97A, and DFP-labeled ClpP (Joshi et al., 2004). Furthermore, ClpX slips back farther and more frequently in the absence of ClpP at the single-molecule level (M.-E. Aubin-Tam et al., 2011; Iosefson, Olivares, et al., 2015; Maillard et al., 2011; Olivares et al., 2017). While the exact mechanisms are unclear, we hypothesize that substrate grip provided by ClpP helps ClpA and ClpX unfold substrate and suppress back slips by ClpX. Our data suggest that ClpP plays a more active role in degradation by aiding in substrate grip that may result in increased degradation efficiency or unfolding speed by preventing reversible folding and premature release. Likewise, the ability of ClpP to grip protein substrates would be predicted to enhance processivity of these proteolytic enzymes by decreasing the probability of substrate release.

3.8 ClpP possibly contributes to processivity

Processive degradation by AAA+ proteases prevents the release of partially degraded products that would be detrimental to cellular function, since these products could bind and inhibit protein partners or lead to aggregation and cell death. However, many AAA+ enzymes are weakly or not processive and do not need to be to fulfill their cellular functions. For example, spastin and katanin only partially unfold tubulin dimers to sever microtubules (Kuo & Howard, 2021), NSF disassembles SNARE complexes without entirely unfolding and translocating individual SNARE proteins (Ryu et al., 2016), and mitochondrial ClpX remodels the heme biosynthetic enzyme ALAS through partial unfolding (Kardon et al., 2020). Despite similarities in structure among the various AAA+ unfoldases characterized to date (Puchades et al., 2020), AAA+ proteases must possess some unique property in order to ensure processive translocation and degradation of substrates. While many studies of ClpXP and ClpAP focus on how the motor contributes to processivity, we propose that the combination of ATPase and peptidase makes a complete processive machine. The ability of the peptidase to perhaps act as a processivity factor is likely a general feature of AAA+ proteases as results from Classen et al. show that the proteasomal 20S core particle also maintains protein substrate grip under load (Classen et al., 2011). However, the 20S active site threonine contributes to the observed mechanical behavior of the enzyme, which we do not observe here for the homologous ClpP active site serine. Therefore, there are likely key differences to how the peptidase components of AAA+ proteases contribute to overall mechanical degradation.

3.9 Sumo-ClpP control experiments

These control experiments were not published with the original work in (Walker & Olivares, 2022), but I am providing them in this dissertation to show a key control for my ClpPS97A mutation. Wild type ClpP has a propeptide sequence that is normally autocatalytically cleaved

(Maurizi, Clark, Katayama, et al., 1990). To express ClpPS97A without a propeptide sequence, I appended an N-terminal sumo domain which is cleaved by the enzyme ULP1, leaving no excess residues. I did this because the propeptide deletion construct would not readily induce in my hands. These data show that cleaved sumo-ClpP-His_6 has similar peptidase activity to the wild type ClpP against FITC-casein and the model CM-titin substrate I used for single molecule studies (Figure 3.8). From these controls, I concluded that the cleaved sumo-ClpP constructs would be suitable to compare against wild type ClpP in optical trapping experiments.

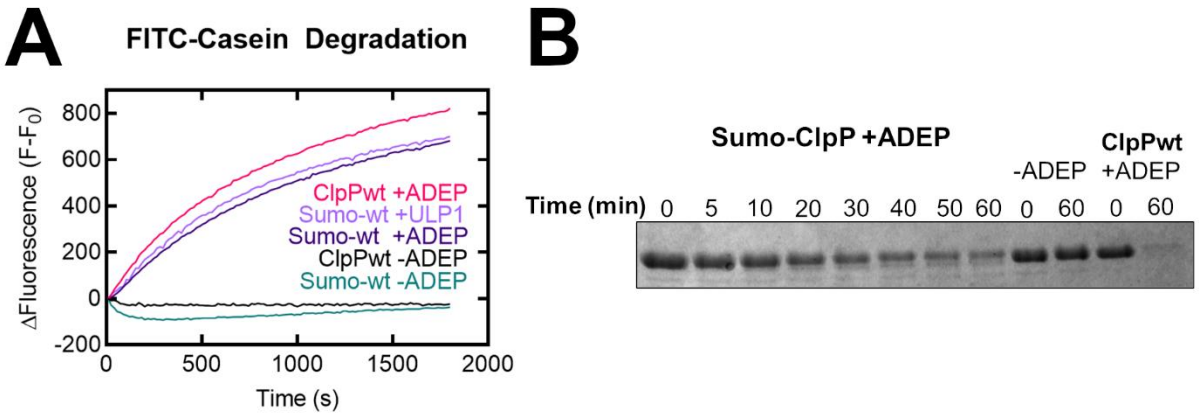

Figure 3.8 Sumo tag expression does not affect ClpP peptidase activity. (A) FITC-casein assay measuring proteolysis over time. Both conditions with sumo degrade FITC-casein similar to wild type ClpP. (B) CM-Titin degradation measured over time by SDS-PAGE. Both the cleaved sumo-ClpP and wild type ClpP degrade CM-titin over the 60 minute time course in an ADEP dependent manner.

CHAPTER 4

Discussion

In my dissertation, I present evidence that ClpP grips a protein substrate against force when activated by ADEP1 and in the absence of any motor proteins. This “holdase” activity by ClpP has not been characterized previously and impacts how we view the function of ClpAP and ClpXP, as well as how we view protein degradation in general by AAA+ proteases. Here I will discuss the impacts that my data have on interpretations of past single molecule experiments and offer several hypotheses for how ClpP grips substrate. Then I will address how ClpP might serve as a model for how the peptidases of AAA+ proteases contribute mechanically to protein degradation in general. Finally, I will *assess* how my data fits into the bigger picture of ADEP biology.

4.1 Implications of ClpP grip in past studies

Almost all the previous single molecule optical tweezers studies of ClpXP and ClpAP included ClpP in their experiments but drew conclusions solely about motor proteins. For example, both the MIT/Vanderbilt and Berkley groups reported ClpX step sizes between 1-4nm for the ClpXP complex (Cordova et al., 2014; Maillard et al., 2011; Sen et al., 2013). Interestingly, the Berkley group noted that 2-3nm bursts were much more frequent than 4nm bursts even at saturating ATP concentrations (Sen et al., 2013), suggesting that some part of the bursts taken by ClpXP did not depend on ATP hydrolysis. Furthermore, the MIT/Vanderbilt group published step sizes of ClpXP and ClpX alone in their first study (M.-E. Aubin-Tam et al., 2011). For ClpXP they observed step sizes of approximately 6.8 and 12.5 amino acids while for ClpX alone they saw 6.8 and 10.5 amino acid steps.

What can account for the differences in bursting behavior and step sizes in these studies? A reasonable hypothesis is that ClpP contributes to these motions through its conformational cycling. The head-to-head distance of the SaClpP tetradecamer changes by 10 angstroms when comparing the extended and compressed conformations (Ye et al., 2013; Zhang et al., 2011, See figure 1.2B). Thus, if ClpP does cycle between conformations when bound to a motor it could contribute up to 1nm to the distances translocated by ClpXP and ClpAP. For the two single molecule examples above, motion by ClpP could help explain the paradoxes in both observations. For example, if the 4nm bursts include 1nm motion by ClpP their frequency would not change with ATP concentration. Furthermore, 1nm is equivalent to approximately 2 amino acids matching the difference in step size between ClpX and ClpXP reported by Aubin-tam and colleagues. While I was unable to see motion by ClpP alone in my experiments, perhaps future single molecule studies will test if ClpP cycles between the extended and compressed conformations during degradation. One method to test such hypotheses could be single molecule FRET.

In addition to step sizes, ClpP could contribute to the degradation mechanics of ClpXP and ClpAP through substrate grip. For example, in solution ClpA unfolds a dimeric protein substrate more slowly than with ClpP present (Baytshtok et al., 2015). Furthermore, ClpXP unfolds GFP more quickly with a longer linker between the substrate and the ssrA degron tag (Martin et al., 2008). If ClpP does grips substrate, this functional grip could impact both mechanical observations. In this dissertation, I showed that activated ClpP gripped a protein substrate against up to 40pN of external force. I also characterized the force dependent lifetimes and estimated an unloaded bond lifetime of approximately 150 seconds. Importantly, this is longer than it takes ClpAP and ClpXP to unfold substrates such as filamin, GFP, and variants of the titin^{I27} domain (M.-E. Aubin-Tam et al., 2011; Cordova et al., 2014; Iosefson, Nager, et al., 2015; Maillard et al., 2011; Olivares et al., 2017; Sen et al., 2013; Shin et al., 2009). Thus, the mechanical activity of activated ClpP happens on force and time scales relevant to both ClpAP and ClpXP, suggesting that ClpP can contribute mechanically to these complexes. To test if ClpP grip contributes to either

ClpXP or ClpAP, one could make mutations in ClpP that affect substrate grip and then test degradation by ClpAP and/or ClpXP. However, the exact mechanism by which ClpP grips protein substrate remains unclear. Therefore, the direct follow up to my research should be to identify what domain(s) and/or residues in ClpP are responsible for substrate grip.

4.2 Structural hypotheses for ClpP substrate grip

In this dissertation, I tested the hypothesis that ClpP grips protein substrate using its active site serine residue. I reasoned that the transient covalent bond formed during peptide hydrolysis might allow ClpP to hold onto protein substrate. Additionally, this idea was shown for the 20S core particle of the proteasome by AFM (Classen et al., 2011). This lab studied rupture forces by the 20S core particle with a casein substrate. The rupture forces for the 20S core particle distributed bimodally, like the ADEP1-ClpP rupture forces presented here; however, Classen and colleagues showed that the active site threonine to alanine mutation decreased the frequency of high force ruptures. In contrast, my data show that mutating the active site serine of ClpP to alanine did not change the distribution of rupture forces (Figure 3.6). Thus, there must be some other mechanism that allows ClpP to grip substrate in a similar manner to the 20S core particle.

What structure(s) in ClpP might be responsible for substrate grip? The next residues I would test are the N-terminal loops of ClpP. For inactive ClpP, these residues occlude the central pore to prevent large/folded substrates from entering, while for active ClpP they are part of the pore lining residues which presumably make important substrate contacts (Effantin et al., 2010; Gribun et al., 2005; Jennings et al., 2008; M. E. Lee et al., 2010). In structural studies, these residues have often shown weak density which suggests flexibility (Sprangers et al., 2005; Wang et al., 1997). When captured in crystal structures, these N-terminal loops were in two distinct orientations which were called the up and down conformations (Bewley et al., 2006; Szyk & Maurizi, 2006). However, in most structures of activated ClpP, by either ADEPs or motor proteins,

the N- terminal loops form ordered β-hairpins that resemble the up conformation (Fei et al., 2020; Li et al., 2010; Lopez et al., 2020; Ripstein et al., 2020; Schmitz et al., 2014). Furthermore, disrupting the structure of these β-hairpins decreases the degradation rate of casein by activated ClpP (Alexopoulos et al., 2013). Overall, the flexibility of the N-terminal loops and their role in substrate gating make these residues candidates for substrate grip. One possibility could be that the N-terminal loops grip substrate strongly in the down conformation and weakly in the up conformation. These two binding modes offer one explanation for the bimodality of my data for both wild type ClpP and ClpPS97A. Furthermore, this mechanism could allow ClpP to act as a Brownian ratchet by preventing backward slipping during strong binding and allowing forward motion during periods of weak binding. If true, this mechanism would also offer an explanation by which ADEP-ClpP unfolds and degrades FtsZ *in vitro* (Sass et al., 2011; Silber et al., 2020).

In addition to the N-terminal loops, other residues within the active site might be necessary and/or work together to confer substrate grip. ClpP uses a canonical Ser-His-Asp catalytic triad to perform peptide hydrolysis (Maurizi, Clark, Katayama, et al., 1990; Maurizi, Clark, Kim, et al., 1990). Perhaps one of catalytic triad residues is more important for grip. In bacterial competition assays and in degradation assays *in vitro*, mutating the active site Asp to Ala was less severe for peptidase activity than mutating the Ser or His residues (Lin et al., 2020). Since the catalytic triad residues affect peptidase activity differently, these residues might also play different roles in substrate binding/grip. Alternatively, it might be necessary to mutate two or more of these residues to significantly affect substrate grip (e.g., a Ser/His double mutant). Additionally, there are non-catalytic residues within the active site that could be responsible for substrate grip. A crystal structure of EcClpP with a covalent inhibitor (benzyloxycarbonyl leucyltyrosine chloromethylketone) shows that Met98, Gly68, Leu125, and Ile70 participate in substrate binding in addition to the active site (Szyk & Maurizi, 2006). These residues might also play a role in substrate grip and would be good candidates to mutate to affect ClpP grip. Ultimately, future

studies of ClpP should focus on the N-terminal loops and other residues within the active site to interrogate the mechanism ClpP uses to forcefully grip protein substrates.

4.3 ClpP: a model for all AAA+ peptidases?

How does substrate grip by ClpP impact how we view other AAA+ proteases? It is possible that peptidase grip contributes to the overall processivity of AAA+ proteases. Generally, processivity is a measure of the amount of time an enzyme translocates along its substrate or track before dissociation. Highly processive enzymes feature out of phase enzymatic cycles between subunits within the machines to ensure that the probability of substrate dissociation is low. Many AAA+ enzymes are not processive. For example, spastin and katanin partially unfold tubulin dimers to sever microtubules (Kuo & Howard, 2021), NSF disassembles snare complexes through partial unfolding (Ryu et al., 2016), and mitochondrial ClpX remodels a heme biosynthetic enzyme through partial unfolding (Kardon et al., 2020). In contrast, AAA+ proteases are highly processive as the release of larger degradation fragments within the cell would be detrimental to life. Thus, there must be some difference in AAA+ proteases to ensure processive translocation and degradation of substrates, despite the high structural similarity between all of the AAA+ enzymes (Puchades et al., 2020).

I propose the peptidase components of AAA+ proteases have additional contributions that have not been accounted for in past studies. Substrate grip by the 20S core particle (Classen et al., 2011) and EcClpP (Walker & Olivares, 2022) provide support for this idea. However, these examples need further characterization and other peptidases should be studied to make a stronger conclusion. Interestingly, AAA+ proteases in bacteria can be divided into two categories where the components are either expressed as separate polypeptides (like ClpP and the 20S core particle), or fused into one polypeptides (like Lon and FtsH) (Olivares et al., 2015). Since both the provided examples are of two component AAA+ proteases, it would be interesting to see

if the peptidases of fused AAA+ proteases also contribute to substrate grip. However, such studies would be more complicated as the AAA+ motor and the peptidase components cannot be studied separately as ClpP and the 20S core particle were. Perhaps substrate grip by the peptidase components further distinguishes these families of AAA+ proteases. Overall, my work characterizing substrate grip by the ClpP peptidase against force raises many questions about past single molecule studies and provides a new perspective for how the field should view mechanical degradation by AAA+ proteases: a cooperative effort between AAA+ motors and their peptidase.

4.4 ClpP grip informs models of ADEP-mediated degradation

Although my dissertation is very focused on the single molecule mechanics of activated ClpP, it does have an impact on our understanding of ADEP biology. It is well established that ADEP binding activates ClpP by opening its central pore, similar to the mechanism that AAA+ motors use to activate ClpP (Brötz-Oesterhelt et al., 2005; Gersch et al., 2015; B.-G. Lee et al., 2010; Li et al., 2010). Furthermore, several *in vitro* studies have characterized that ADEP-activated ClpP likely degrades nascent polypeptide chains in cells (Brötz-Oesterhelt et al., 2005; Kirstein et al., 2009), and in prokaryotes the cell division protein FtsZ (Sass et al., 2011; Silber et al., 2020). These activities ultimately cause cell death for both prokaryotic and eukaryotic cells, showing promise as an antibiotic in mice against *S. aureus* infection (Conlon et al., 2013) and as anti-cancer agents in humans (Graves et al., 2019; Wong & Houry, 2019). However, what remains unclear is the mechanism by which ADEP-ClpP chooses specific targets.

For example, Brötz-Oesterhelt and colleagues used 2-D gel electrophoresis to show that ADEP-ClpP partially degraded several bacterial proteins like DnaK, Trigger Factor, and Ef-Tu in *Bacillus subtilis* cells (Brötz-Oesterhelt et al., 2005). Additionally, Conlon and colleagues used proteomics to show that ADEP-ClpP partially degrades several proteins in addition to the findings

from Brötz-Oesterhelt and colleagues, and that ADEP-ClpP fully degrades other protein targets in *S. aureus* cells (Conlon et al., 2013). Taken together, these data demonstrate that ADEP-ClpP targets certain proteins more than others and even has differential degradation of these targets. However, the current model of indiscriminate proteolysis, including nascent chains, fails to explain why ADEP-ClpP has specific targets in cells and why it shows differential treatment. While my data do not offer an alternative model, I will offer next steps to improving our mechanistic understanding of ADEP biology.

The data in this dissertation show that ADEP-ClpP maintains grip on a model substrate for hundreds of seconds in the absence of applied force. I hypothesize that the cellular targets of ADEP-ClpP depend on its ability to grip specific motifs in each substrate, and if it has strong enough grip possibly unfold them to for complete degradation. While Conlon and colleagues performed a proteomic analysis of ADEP-ClpP, an intersting study to complement those data would be co-immunoprecipitation of inactive ADEP-ClpP. My data suggest that ADEP-ClpP grips protein substrate strongly enough to co-purify substrates from cells, and co-immunopreciptation would provide insight into which proteins bind ADEP-ClpP more abundantly in a cellular context. It might also clarify if ADEP-ClpP relies on any chaperones to help it target proteins, as ClpXP has been shown to cooperate with trigger factor (Rizzolo et al., 2021). It is possible that since ADEPs are competive inhibitors of the native ClpP-motor interactions, perhaps ADEP-ClpP causes a change that allows ClpP to functionally cooperate with other chaperones to help degrade other substrates within the cell. Overall, this disseration provides a new perspective regarding the targeting of specific substrates by ADEP-ClpP.

References

Alexopoulos, J., Ahsan, B., Homchaudhuri, L., Husain, N., Cheng, Y. Q., & Ortega, J. (2013). Structural determinants stabilizing the axial channel of ClpP for substrate translocation. *Molecular Microbiology*, *90*(1), 167–180. https://doi.org/10.1111/mmi.12356

Amor, A. J., Schmitz, K. R., Sello, J. K., Baker, T. A., & Sauer, R. T. (2016). Highly Dynamic Interactions Maintain Kinetic Stability of the ClpXP Protease during the ATP-Fueled Mechanical Cycle. *ACS Chemical Biology*, *11*(6), 1552–1560. https://doi.org/10.1021/acschembio.6b00083

Aubin-Tam, M.-E., Olivares, A. O., Sauer, R. T., Baker, T. A., & Lang, M. J. (2011). Single-Molecule Protein Unfolding and Translocation by an ATP-Fueled Proteolytic Machine. *Cell*, *145*(2), 257–267. https://doi.org/10.1016/J.CELL.2011.03.036

Aubin-Tam, M. E., Appleyard, D. C., Ferrari, E., Garbin, V., Fadiran, O. O., Kunkel, J., & Lang, M. J. (2011). Adhesion through single peptide aptamers. *Journal of Physical Chemistry A*, *115*(16), 3657–3664. https://doi.org/10.1021/jp1031493

Barkow, S. R., Levchenko, I., Baker, T. A., & Sauer, R. T. (2009). Polypeptide Translocation by the AAA+ ClpXP Protease Machine. *Chemistry & Biology*, *16*(6), 605–612. https://doi.org/10.1016/J.CHEMBIOL.2009.05.007

Baytshtok, V., Baker, T. A., & Sauer, R. T. (2015). Mechanism of protein remodeling by ClpA chaperone. *Proceedings of the National Academy of Sciences*, *112*(17), 5377–5382. https://doi.org/10.1073/pnas.94.10.4901

Bell, G. I. (1978). Models for the specific adhesion of cells to cells. *Science*, *200*(4342), 618 LP – 627. https://doi.org/10.1126/science.347575

Bewley, M. C., Graziano, V., Griffin, K., & Flanagan, J. M. (2006). The asymmetry in the mature amino-terminus of ClpP facilitates a local symmetry match in ClpAP and ClpXP complexes. *Journal of Structural Biology*, *153*(2), 113–128.

https://doi.org/https://doi.org/10.1016/j.jsb.2005.09.011

Bhandari, V., Wong, K. S., Zhou, J. L., Mabanglo, M. F., Batey, R. A., & Houry, W. A. (2018). The Role of ClpP Protease in Bacterial Pathogenesis and Human Diseases [Review-article]. *ACS Chemical Biology*, *13*(6), 1413–1425. https://doi.org/10.1021/acschembio.8b00124

Brodie, E. J., Zhan, H., Saiyed, T., Truscott, K. N., & Dougan, D. A. (2018). Perrault syndrome type 3 caused by diverse molecular defects in CLPP. *Scientific Reports*, *8*(1), 1–11. https://doi.org/10.1038/s41598-018-30311-1

Brötz-Oesterhelt, H., Beyer, D., Kroll, H. P., Endermann, R., Ladel, C., Schroeder, W., Hinzen, B., Raddatz, S., Paulsen, H., Henninger, K., Bandow, J. E., Sahl, H. G., & Labischinski, H. (2005). Dysregulation of bacterial proteolytic machinery by a new class of antibiotics. *Nature Medicine*, *11*(10), 1082–1087. https://doi.org/10.1038/nm1306

Burton, R. E., Siddiqui, S. M., Kim, Y. I., Baker, T. A., & Sauer, R. T. (2001). Effects of protein stability and structure on substrate processing by the ClpXP unfolding and degradation machine. *EMBO Journal*, *20*(12), 3092–3100. https://doi.org/10.1093/emboj/20.12.3092

Bustamante, C. J., Chemla, Y. R., Liu, S., & Wang, M. D. (2021). Optical tweezers in single-molecule biophysics. *Nature Reviews Methods Primers*, *1*. https://doi.org/10.1038/s43586-021-00021-6

Classen, M., Breuer, S., Baumeister, W., Guckenberger, R., & Witt, S. (2011). Force spectroscopy of substrate molecules en route to the proteasome's active sites. *Biophysical Journal*, *100*(2), 489–497. https://doi.org/10.1016/j.bpj.2010.12.3689

Conlon, B. P., Nakayasu, E. S., Fleck, L. E., Lafleur, M. D., Isabella, V. M., Coleman, K., Leonard, S. N., Smith, R. D., Adkins, J. N., & Lewis, K. (2013). Activated ClpP kills persisters and eradicates a chronic biofilm infection. *Nature*, *503*(7476), 365–370. https://doi.org/10.1038/nature12790

Cordova, J. C., Olivares, A. O., & Lang, M. J. (2017). Mechanically watching the ClpXP

proteolytic machinery. In *Methods in Molecular Biology* (Vol. 1486, pp. 317–341). Humana Press Inc. https://doi.org/10.1007/978-1-4939-6421-5_12

Cordova, J. C., Olivares, A. O., Shin, Y., Stinson, B. M., Calmat, S., Schmitz, K. R., Aubin-Tam, M. E., Baker, T. A., Lang, M. J., & Sauer, R. T. (2014). Stochastic but highly coordinated protein unfolding and translocation by the ClpXP proteolytic machine. *Cell*, *158*, 647–658. https://doi.org/10.1016/j.cell.2014.05.043

Dudko, O. K., Hummer, G., & Szabo, A. (2006). Intrinsic rates and activation free energies from single-molecule pulling experiments. *Physical Review Letters*, *96*(10), 1–4. https://doi.org/10.1103/PhysRevLett.96.108101

Effantin, G., Maurizi, M. R., & Steven, A. C. (2010). Binding of the ClpA Unfoldase Opens the Axial Gate of ClpP Peptidase. *Journal of Biological Chemistry* , *285*(19), 14834–14840. https://doi.org/10.1074/jbc.M109.090498

Evans, E., & Ritchie, K. (1997). Dynamic Strength of Molecular Adhesion Bonds. *Biophysical Journal*, *72*(4), 1541–1555. https://doi.org/10.1016/S0006-3495(97)78802-7

Fei, X., Bell, T. A., Jenni, S., Stinson, B. M., Baker, T. A., Harrison, S. C., & Sauer, R. T. (2020). Structures of the ATP-fueled ClpXP proteolytic machine bound to protein substrate. *ELife*, *9*. https://doi.org/10.7554/eLife.52774

Feng, J., Michalik, S., Varming, A. N., Andersen, J. H., Albrecht, D., Jelsbak, L., Krieger, S., Ohlsen, K., Hecker, M., Gerth, U., Ingmer, H., & Frees, D. (2013). Trapping and proteomic identification of cellular substrates of the ClpP protease in staphylococcus aureus. *Journal of Proteome Research*, *12*(2), 547–558. https://doi.org/10.1021/pr300394r

Flynn, J. M., Neher, S. B., Kim, Y.-I., Sauer, R. T., & Baker, T. A. (2003). Proteomic Discovery of Cellular Substrates of the ClpXP Protease Reveals Five Classes of ClpX-Recognition Signals. *Molecular Cell*, *11*(3), 671–683. https://doi.org/https://doi.org/10.1016/S1097-2765(03)00060-1

Gaillot, O., Pellegrini, E., Bregenholt, S., Nair, S., & Berche, P. (2000). The ClpP serine

protease is essential for the intracellular parasitism and virulence of Listeria monocytogenes. In *Molecular Microbiology* (Issue 6).

Gates, S. N., & Martin, A. (2020). Stairway to translocation: AAA+ motor structures reveal the mechanisms of ATP-dependent substrate translocation. In *Protein Science* (Vol. 29, Issue 2, pp. 407–419). Blackwell Publishing Ltd. https://doi.org/10.1002/pro.3743

Geiger, S. R., Böttcher, T., Sieber, S. A., & Cramer, P. (2011). A conformational switch underlies ClpP protease function. *Angewandte Chemie - International Edition*, *50*(25), 5749–5752. https://doi.org/10.1002/anie.201100666

Gersch, M., Famulla, K., Dahmen, M., Göbl, C., Malik, I., Richter, K., Korotkov, V. S., Sass, P., Rübsamen-Schaeff, H., Madl, T., Brötz-Oesterhelt, H., & Sieber, S. A. (2015). AAA+ chaperones and acyldepsipeptides activate the ClpP protease via conformational control. *Nature Communications*, *6*(1), 6320. https://doi.org/10.1038/ncomms7320

Gersch, M., List, A., Groll, M., & Sieber, S. A. (2012). Insights into structural network responsible for oligomerization and activity of bacterial virulence regulator caseinolytic protease P (ClpP) protein. *Journal of Biological Chemistry*, *287*(12), 9484–9494. https://doi.org/10.1074/jbc.M111.336222

Graves, P. R., Aponte-Collazo, L. J., Fennell, E. M. J., Graves, A. C., Hale, A. E., Dicheva, N., Herring, L. E., Gilbert, T. S. K., East, M. P., McDonald, I. M., Lockett, M. R., Ashamalla, H., Moorman, N. J., Karanewsky, D. S., Iwanowicz, E. J., Holmuhamedov, E., & Graves, L. M. (2019). Mitochondrial Protease ClpP is a Target for the Anticancer Compounds ONC201 and Related Analogues. *ACS Chemical Biology*, *14*(5), 1020–1029. https://doi.org/10.1021/acschembio.9b00222

Gribun, A., Kimber, M. S., Ching, R., Sprangers, R., Fiebig, K. M., & Houry, W. A. (2005). The ClpP double ring tetradecameric protease exhibits plastic ring-ring interactions, and the N termini of its subunits form flexible loops that are essential for ClpXP and ClpAP complex formation. *Journal of Biological Chemistry*, *280*(16), 16185–16196.

https://doi.org/10.1074/jbc.M414124200

Hinnerwisch, J., Reid, B. G., Fenton, W. A., & Horwich, A. L. (2005). Roles of the N-domains of the ClpA unfoldase in binding substrate proteins and in stable complex formation with the ClpP protease. *Journal of Biological Chemistry*, *280*(49), 40838–40844. https://doi.org/10.1074/jbc.M507879200

Hipp, M. S., Kasturi, P., & Hartl, F. U. (2019). The proteostasis network and its decline in ageing. *Nature Reviews Molecular Cell Biology*, *20*(7), 421–435. https://doi.org/10.1038/s41580-019-0101-y

Ingvarsson, H., Maté, M. J., Högbom, M., Portnoï, D., Benaroudj, N., Alzari, P. M., Ortiz-Lombardía, M., & Unge, T. (2007). Insights into the inter-ring plasticity of caseinolytic proteases from the X-ray structure of Mycobacterium tuberculosis ClpP1. *Acta Crystallographica Section D: Biological Crystallography*, *63*(2), 249–259. https://doi.org/10.1107/S0907444906050530

Iosefson, O., Nager, A. R., Baker, T. A., & Sauer, R. T. (2015). Coordinated gripping of substrate by subunits of a AAA+ proteolytic machine. *Nature Chemical Biology*, *11*(3), 201–206. https://doi.org/10.1038/nchembio.1732

Iosefson, O., Olivares, A. O., Baker, T. A., & Sauer, R. T. (2015). Dissection of axial-pore loop function during unfolding and translocation by a AAA+ proteolytic machine. *Cell Reports*, *12*, 1032–1041. https://doi.org/10.1016/j.celrep.2015.07.007

Jenal, U., & Fuchs, T. (1998). An essential protease involved in bacterial cell-cycle control. *EMBO Journal*, *17*(19), 5658–5669. https://doi.org/10.1093/emboj/17.19.5658

Jenkinson, E. M., Rehman, A. U., Walsh, T., Clayton-Smith, J., Lee, K., Morell, R. J., Drummond, M. C., Khan, S. N., Naeem, M. A., Rauf, B., Billington, N., Schultz, J. M., Urquhart, J. E., Lee, M. K., Berry, A., Hanley, N. A., Mehta, S., Cilliers, D., Clayton, P. E., … Newman, W. G. (2013). Perrault syndrome is caused by recessive mutations in CLPP, encoding a mitochondrial ATP-dependent chambered protease. *American Journal of*

Human Genetics, *92*(4), 605–613. https://doi.org/10.1016/j.ajhg.2013.02.013

Jennings, L. D., Bohon, J., Chance, M. R., & Licht, S. (2008). The ClpP N-terminus coordinates substrate access with protease active site reactivity. *Biochemistry*, *47*(42), 11031–11040. https://doi.org/10.1021/bi8010169

Joshi, S. A., Hersch, G. L., Baker, T. A., & Sauer, R. T. (2004). Communication between ClpX and ClpP during substrate processing and degradation. *Nature Structural and Molecular Biology*, *11*(5), 404–411. https://doi.org/10.1038/nsmb752

Kang, S. G., Maurizi, M. R., Thompson, M., Mueser, T., & Ahvazi, B. (2004). Crystallography and mutagenesis point to an essential role for the N-terminus of human mitochondrial ClpP. *Journal of Structural Biology*, *148*, 338–352. https://doi.org/10.1016/j.jsb.2004.07.004

Kardon, J. R., Moroco, J. A., Engen, J. R., & Baker, T. A. (2020). Mitochondrial clpx activates an essential biosynthetic enzyme through partial unfolding. *ELife*, *9*, 1–20. https://doi.org/10.7554/eLife.54387

Kenniston, J. A., Baker, T. A., Fernandez, J. M., & Sauer, R. T. (2003). Linkage between ATP consumption and mechanical unfolding during the protein processing reactions of an AAA+ degradation machine. *Cell*, *114*(4), 511–520. https://doi.org/10.1016/S0092-8674(03)00612-3

Kim, Y. I., Burton, R. E., Burton, B. M., Sauer, R. T., & Baker, T. A. (2000). Dynamics of substrate denaturation and translocation by the ClpXP degradation machine. *Molecular Cell*, *5*(4), 639–648. https://doi.org/10.1016/S1097-2765(00)80243-9

Kim, Y. I., Levchenko, I., Fraczkowska, K., Woodruff, R. V., Sauer, R. T., & Baker, T. A. (2001). Molecular determinants of complex formation between Clp/Hsp 100 ATPases and the ClpP peptidase. *Nature Structural Biology*, *8*(3), 230–233. https://doi.org/10.1038/84967

Kimber, M. S., Yu, A. Y. H., Borg, M., Leung, E., Chan, H. S., & Houry, W. A. (2010). Structural and Theoretical Studies Indicate that the Cylindrical Protease ClpP Samples Extended and Compact Conformations. *Structure*, *18*, 798–808. https://doi.org/10.1016/j.str.2010.04.008

Kirstein, J., Hoffmann, A., Lilie, H., Schmidt, R., Helga, R. W., Heike, B. O., Mogk, A., & Turgay, K. (2009). The antibiotic ADEP reprogrammes ClpP, switching it from a regulated to an uncontrolled protease. *EMBO Molecular Medicine*, *1*(1), 37–49. https://doi.org/10.1002/emmm.200900002

Klaips, C. L., Jayaraj, G. G., & Hartl, F. U. (2017). Pathways of cellular proteostasis in aging and disease. *Journal of Cell Biology*, *217*(1), 51–63. https://doi.org/10.1083/jcb.201709072

Kock, H., Gerth, U., & Hecker, M. (2004). *The ClpP Peptidase Is the Major Determinant of Bulk Protein Turnover in Bacillus subtilis*. *186*(17), 5856–5864. https://doi.org/10.1128/JB.186.17.5856

Kotamarthi, H. C., Sauer, R. T., & Baker, T. A. (2020). The Non-dominant AAA+ Ring in the ClpAP Protease Functions as an Anti-stalling Motor to Accelerate Protein Unfolding and Translocation. *Cell Reports*, *30*(8), 2644-2654.e3. https://doi.org/10.1016/j.celrep.2020.01.110

Kuo, Y. W., & Howard, J. (2021). Cutting, Amplifying, and Aligning Microtubules with Severing Enzymes. *Trends in Cell Biology*, *31*(1), 50–61. https://doi.org/10.1016/j.tcb.2020.10.004

Kurtishi, A., Rosen, B., Patil, K. S., Alves, G. W., & Møller, S. G. (2019). Cellular Proteostasis in Neurodegeneration. *Molecular Neurobiology*, *56*(5), 3676–3689. https://doi.org/10.1007/s12035-018-1334-z

Lang, M. J., Fordyce, P. M., Fordyce, A. M., Neuman, K. C., & Block, S. M. (2004). Simultaneous, coincident optical trapping and single-molecule fluorescence. *Nature Methods*, *1*(2), 133–139. https://doi.org/10.1038/nmeth714

Lee, B.-G., Park, E. Y., Lee, K.-E., Jeon, H., Sung, K. H., Paulsen, H., Rübsamen-Schaeff, H., Brötz-Oesterhelt, H., & Song, H. K. (2010). Structures of ClpP in complex with acyldepsipeptide antibiotics reveal its activation mechanism. *Nature Structural &Amp; Molecular Biology*, *17*, 471. https://doi.org/10.1038/nsmb.1787

Lee, M. E., Baker, T. A., & Sauer, R. T. (2010). Control of substrate gating and translocation into

ClpP by channel residues and ClpX binding. *Journal of Molecular Biology*, *399*(5), 707–718. https://doi.org/10.1016/j.jmb.2010.04.027

Li, D. H. S., Chung, Y. S., Gloyd, M., Joseph, E., Ghirlando, R., Wright, G. D., Cheng, Y.-Q., Maurizi, M. R., Guarné, A., & Ortega, J. (2010). Acyldepsipeptide Antibiotics Induce the Formation of a Structured Axial Channel in ClpP: A Model for the ClpX/ClpA-Bound State of ClpP. *Chemistry & Biology*, *17*(9), 959–969. https://doi.org/10.1016/J.CHEMBIOL.2010.07.008

Lin, H.-H., Yu, M., Sriramoju, M. K., Hsu, S.-T. D., Liu, C.-T., & Lai, E.-M. (2020). A High-Throughput Interbacterial Competition Screen Identifies ClpAP in Enhancing Recipient Susceptibility to Type VI Secretion System-Mediated Attack by Agrobacterium tumefaciens . In *Frontiers in Microbiology* (Vol. 10). https://www.frontiersin.org/articles/10.3389/fmicb.2019.03077

Lopez, K. E., Rizo, A. N., Tse, E., Lin, J., Scull, N. W., Thwin, A. C., Lucius, A. L., Shorter, J., & Southworth, D. R. (2020). Conformational plasticity of the ClpAP AAA+ protease couples protein unfolding and proteolysis. *Nature Structural & Molecular Biology*, *27*(5), 406–416. https://doi.org/10.1038/s41594-020-0409-5

Mabanglo, M. F., & Houry, W. A. (2022). Recent structural insights into the mechanism of ClpP protease regulation by AAA+ chaperones and small molecules. *Journal of Biological Chemistry*, 101781. https://doi.org/10.1016/j.jbc.2022.101781

Maillard, R. A., Chistol, G., Sen, M., Righini, M., Tan, J., Kaiser, C. M., Hodges, C., Martin, A., & Bustamante, C. (2011). ClpX(P) generates mechanical force to unfold and translocate its protein substrates. *Cell*, *145*, 459–469. https://doi.org/10.1016/j.cell.2011.04.010

Malik, I. T., & Brötz-Oesterhelt, H. (2017). Conformational control of the bacterial Clp protease by natural product antibiotics. *Natural Product Reports*, *34*(7), 815–831. https://doi.org/10.1039/c6np00125d

Martin, A., Baker, T. A., & Sauer, R. T. (2008). Protein unfolding by a AAA+ protease is

dependent on ATP-hydrolysis rates and substrate energy landscapes. *Nature Structural and Molecular Biology*, *15*(2), 139–145. https://doi.org/10.1038/nsmb.1380

Martín, Á. S., Rodriguez-Aliaga, P., Molina, J. A., Martin, A., Bustamante, C., & Baez, M. (2017). Knots can impair protein degradation by ATP-dependent proteases. *Proceedings of the National Academy of Sciences of the United States of America*, *114*(37), 9864–9869. https://doi.org/10.1073/pnas.1705916114

Maurizi, M. R., Clark, W. P., Katayama, Y., Rudikoff, S., Pumphrey, J., Bowers, B., & Gottesman, S. (1990). Sequence and structure of Clp P, the proteolytic component of the ATP-dependent Clp protease of Escherichia coli. *Journal of Biological Chemistry* , *265*(21), 12536–12545. http://www.jbc.org/content/265/21/12536.abstract

Maurizi, M. R., Clark, W. P., Kim, S. H., & Gottesman, S. (1990). Clp P represents a unique family of serine proteases. *Journal of Biological Chemistry*, *265*(21), 12546–12552.

Merkel, R., Nassoy, P., Leung, A., Ritchie, K., & Evans, E. (1999). Energy landscapes of receptor-ligand bonds explored with dynamic force spectroscopy. *Nature*, *397*(6714), 50–53. https://doi.org/10.1038/16219

Miller, J. M., Lin, J., Li, T., & Lucius, A. L. (2013). E. coli ClpA catalyzed polypeptide translocation is allosterically controlled by the protease ClpP. *Journal of Molecular Biology*, *425*, 2795–2812. https://doi.org/10.1016/j.jmb.2013.04.019

Moffitt, J. R., Chemla, Y. R., Smith, S. B., & Bustamante, C. (2008). Recent Advances in Optical Tweezers. *Annual Review of Biochemistry*, *77*(1), 205–228. https://doi.org/10.1146/annurev.biochem.77.043007.090225

Moreno-cinos, C., Goossens, K., Salado, I. G., & Veken, P. Van Der. (2019). ClpP Protease , a Promising Antimicrobial Target. *International Journal of Molecular Sciences*, *20*(9). https://doi.org/https://doi.org/10.3390/ijms20092232

Nager, A. R., Baker, T. A., & Sauer, R. T. (2011). Stepwise unfolding of a β barrel protein by the AAA+ ClpXP protease. *Journal of Molecular Biology*, *413*, 4–16.

https://doi.org/10.1016/j.jmb.2011.07.041

Neher, S. B., Villén, J., Oakes, E. C., Bakalarski, C. E., Sauer, R. T., Gygi, S. P., & Baker, T. A. (2006). Proteomic Profiling of ClpXP Substrates after DNA Damage Reveals Extensive Instability within SOS Regulon. *Molecular Cell*, *22*(2), 193–204. https://doi.org/10.1016/j.molcel.2006.03.007

Neuert, G., Albrecht, C., Pamir, E., & Gaub, H. E. (2006). Dynamic force spectroscopy of the digoxigenin-antibody complex. *FEBS Letters*, *580*(2), 505–509. https://doi.org/10.1016/j.febslet.2005.12.052

Neuman, K. C., & Block, S. M. (2004). Optical trapping. *Physics Today*, *75*(9), 2787–2809. https://doi.org/10.1063/1.2408485

Olivares, A. O., Baker, T. A., & Sauer, R. T. (2015). Mechanistic insights into bacterial AAA+ proteases and protein-remodelling machines. *Nature Reviews Microbiology*, *14*(1), 33–44. https://doi.org/10.1038/nrmicro.2015.4

Olivares, A. O., Baker, T. A., & Sauer, R. T. (2018). Mechanical Protein Unfolding and Degradation. *Annual Review of Physiology*, *80*(1), 413–429. https://doi.org/10.1146/annurev-physiol-021317-121303

Olivares, A. O., Kotamarthi, H. C., Stein, B. J., Sauer, R. T., & Baker, T. A. (2017). Effect of directional pulling on mechanical protein degradation by ATP-dependent proteolytic machines. *Proceedings of the National Academy of Sciences*, *114*(31), E6306 LP-E6313. https://doi.org/10.1073/pnas.1707794114

Olivares, A. O., Nager, A. R., Iosefson, O., Sauer, R. T., & Baker, T. A. (2014). Mechanochemical basis of protein degradation by a double-ring AAA+ machine. *Nature Structural and Molecular Biology*, *21*(10), 871–875. https://doi.org/10.1038/nsmb.2885

Peterson, C. N., Levchenko, I., Rabinowitz, J. D., Baker, T. A., & Silhavy, T. J. (2012). RpoS proteolysis is controlled directly by ATP levels in Escherichia coli. *Genes and Development*, *26*(6), 548–553. https://doi.org/10.1101/GAD.183517.111

Puchades, C., Sandate, C. R., & Lander, G. C. (2020). The molecular principles governing the activity and functional diversity of AAA+ proteins. In *Nature Reviews Molecular Cell Biology* (Vol. 21, Issue 1, pp. 43–58). https://doi.org/10.1038/s41580-019-0183-6

Rajendar, B., & Lucius, A. L. (2010). Molecular mechanism of polypeptide translocation catalyzed by the Escherichia coli ClpA Protein Translocase. *Journal of Molecular Biology*, *399*(5), 665–679. https://doi.org/10.1016/j.jmb.2010.03.061

Ripstein, Z. A., Vahidi, S., Houry, W. A., Rubinstein, J. L., & Kay, L. E. (2020). A processive rotary mechanism couples substrate unfolding and proteolysis in the ClpXP degradation machinery. *ELife*, *9*. https://doi.org/10.7554/eLife.52158

Rizzolo, K., Yu, A. Y. H., Ologbenla, A., Kim, S. R., Zhu, H., Ishimori, K., Thibault, G., Leung, E., Zhang, Y. W., Teng, M., Haniszewski, M., Miah, N., Phanse, S., Minic, Z., Lee, S., Caballero, J. D., Babu, M., Tsai, F. T. F., Saio, T., & Houry, W. A. (2021). Functional cooperativity between the trigger factor chaperone and the ClpXP proteolytic complex. *Nature Communications*, *12*(1), 1–18. https://doi.org/10.1038/s41467-020-20553-x

Rodriguez-Aliaga, P., Ramirez, L., Kim, F., Bustamante, C., & Martin, A. (2016). Substrate-translocating loops regulate mechanochemical coupling and power production in AAA+ protease ClpXP. *Nature Structural & Molecular Biology*, *23*(11), 974–981. https://doi.org/10.1038/nsmb.3298

Romberg, L., Levin, P. A., & Drive, O. B. (2017). Poised at the Edge of Stability. *Annual Review of Microbiology*, *57*, 125–154. https://doi.org/10.1146/annurev.micro.57.012903.074300.Assembly

Ryu, J. K., Jahn, R., & Yoon, T. Y. (2016). Review: Progresses in understanding N-ethylmaleimide sensitive factor (NSF) mediated disassembly of SNARE complexes. *Biopolymers*, *105*(8), 518–531. https://doi.org/10.1002/bip.22854

Sass, P., Josten, M., Famulla, K., Schiffer, G., Sahl, H.-G., Hamoen, L., & Brötz-Oesterhelt, H. (2011). Antibiotic acyldepsipeptides activate ClpP peptidase to degrade the cell division

protein FtsZ. *Proceedings of the National Academy of Sciences*, *108*(42), 17474–17479. https://doi.org/10.1073/PNAS.1110385108

Schmitz, K. R., Carney, D. W., Sello, J. K., & Sauer, R. T. (2014). Crystal structure of mycobacterium tuberculosis ClpP1p2 suggests a model for peptidase activation by aaa+ partner binding and substrate delivery. *Proceedings of the National Academy of Sciences of the United States of America*, *111*(43), E4587–E4595. https://doi.org/10.1073/pnas.1417120111

Sen, M., Maillard, R. A., Nyquist, K., Rodriguez-Aliaga, P., Pressé, S., Martin, A., & Bustamante, C. (2013). The ClpXP protease unfolds substrates using a constant rate of pulling but different gears. *Cell*, *155*, 636–646. https://doi.org/10.1016/j.cell.2013.09.022

Shin, Y., Davis, J. H., Brau, R. R., Martin, A., Kenniston, J. A., Baker, T. A., Sauer, R. T., & Lang, M. J. (2009). Single-molecule denaturation and degradation of proteins by the AAA+ ClpXP protease. *Proceedings of the National Academy of Sciences*, *106*(46), 19340–19345. https://doi.org/10.1073/pnas.0910484106

Silber, N., Pan, S., Schäkermann, S., Mayer, C., Brötz-Oesterhelt, H., & Sass, P. (2020). Cell Division Protein FtsZ Is Unfolded for N-Terminal Degradation by Antibiotic-Activated ClpP. *MBio*, *11*(3), e01006-20. https://doi.org/10.1128/mBio.01006-20

Sivertsson, E. M., Jackson, S. E., & Itzhaki, L. S. (2019). The AAA+ protease ClpXP can easily degrade a 3 1 and a 5 2 -knotted protein. *Scientific Reports*, *9*(1), 1–14. https://doi.org/10.1038/s41598-018-38173-3

Sprangers, R., Gribun, A., Hwang, P. M., Houry, W. A., & Kay, L. E. (2005). Quantitative NMR spectroscopy of supramolecular complexes: Dynamic side pores in ClpP are important for product release. *Proceedings of the National Academy of Sciences of the United States of America*, *102*(46), 16678–16683. https://doi.org/10.1073/pnas.0507370102

Sriramoju, M. K., Chen, Y., Lee, Y. T. C., & Hsu, S. T. D. (2018). Topologically knotted deubiquitinases exhibit unprecedented mechanostability to withstand the proteolysis by an

AAA+ protease. *Scientific Reports*, *8*(1), 1–9. https://doi.org/10.1038/s41598-018-25470-0

Stinson, B. M., Baytshtok, V., Schmitz, K. R., Baker, T. A., & Sauer, R. T. (2015). Subunit asymmetry and roles of conformational switching in the hexameric AAA+ ring of ClpX. *Nature Structural & Molecular Biology*, *22*, 411. https://doi.org/10.1038/nsmb.3012

Szyk, A., & Maurizi, M. R. (2006). Crystal structure at 1.9Å of E. coli ClpP with a peptide covalently bound at the active site. *Journal of Structural Biology*, *156*(1), 165–174. https://doi.org/https://doi.org/10.1016/j.jsb.2006.03.013

Thompson, M. W., Singh, S. K., & Maurizi, M. R. (1994). Processive degradation of proteins by the ATP-dependent Clp protease from Escherichia coli. Requirement for the multiple array of active sites in ClpP but not ATP hydrolysis. *Journal of Biological Chemistry*, *269*(27), 18209–18215. https://doi.org/https://doi.org/10.1016/S0021-9258(17)32436-5

Walker, S. D., & Olivares, A. O. (2022). The activated ClpP peptidase forcefully grips a protein substrate. *Biophysical Journal*, *121*(3), 21a. https://doi.org/10.1016/j.bpj.2021.11.2600

Wang, J., Hartling, J. A., & Flanagan, J. M. (1997). The structure of ClpP at 2.3 Å resolution suggests a model for ATP- dependent proteolysis. *Cell*, *91*, 447–456. https://doi.org/10.1016/S0092-8674(00)80431-6

Wong, K. S., & Houry, W. A. (2019). Chemical Modulation of Human Mitochondrial ClpP: Potential Application in Cancer Therapeutics. *ACS Chemical Biology*. https://doi.org/10.1021/acschembio.9b00347

Wong, K. S., Mabanglo, M. F., Seraphim, T. V., Mollica, A., Mao, Y.-Q., Rizzolo, K., Leung, E., Moutaoufik, M. T., Hoell, L., Phanse, S., Goodreid, J., Barbosa, L. R. S., Ramos, C. H. I., Babu, M., Mennella, V., Batey, R. A., Schimmer, A. D., & Houry, W. A. (2018). Acyldepsipeptide Analogs Dysregulate Human Mitochondrial ClpP Protease Activity and Cause Apoptotic Cell Death. *Cell Chemical Biology*, *25*(8), 1017–1030. https://doi.org/10.1016/J.CHEMBIOL.2018.05.014

Ye, F., Li, J., & Yang, C. G. (2017). The development of small-molecule modulators for ClpP

protease activity. *Molecular BioSystems*, *13*(1), 23–31. https://doi.org/10.1039/C6MB00644B

Ye, F., Zhang, J., Hilgenfeld, R., Li, D., Zhang, X., Jiang, H., Zhang, R., Yang, C.-G., Li, L., Luo, C., Lu, J., Kong, X., & Liu, H. (2013). Helix Unfolding/Refolding Characterizes the Functional Dynamics of Staphylococcus aureus Clp Protease. *Journal of Biological Chemistry*, *288*(24), 17643–17653. https://doi.org/10.1074/jbc.m113.452714

Yu, A. Y. H., & Houry, W. A. (2007). ClpP: A distinctive family of cylindrical energy-dependent serine proteases. *FEBS Letters*, *581*(19), 3749–3757. https://doi.org/10.1016/j.febslet.2007.04.076

Zhang, J., Ye, F., Lan, L., Jiang, H., Luo, C., & Yang, C. G. (2011). Structural switching of Staphylococcus aureus Clp protease: A key to understanding protease dynamics. *Journal of Biological Chemistry*, *286*(43), 37590–37601. https://doi.org/10.1074/jbc.M111.277848

APPENDIX A

Protocols and Codes

Expression and Purification of ClpP-His_6-Cys

Materials

Production and Expression:
- Amp media plates *(in cold room stock)*
- LB Media *(from stock at RT)*
- 1000x Amp *(stocks stored at -20C)*
- 1M IPTG *(stocks stored at -20C)*
- 18% SDS-PAGE gels *(will need at least 4)*

Stock Buffer (2x):
pH 8.0 (100mM sodium phosphate, 2M NaCl, 20% glycerol)
To make 500mL:
2.98mL of 1M NaH_2PO_4
94mL of 0.5M Na_2HPO_4
58.44g NaCl
100mL glycerol
Add ddH_2O to total volume 500mL and adjust pH to 8.0.

Lysis and Binding:
S buffer: pH 8.0 (50mM sodium phosphate, 1M NaCl, 5mM imidazole, 10% glycerol)
To make 500mL:
250mL 2x stock buffer
2.5mL 1M imidazole *(stored in dark at 4C)*
247.5 mL ddH_2O

Wash Buffer:
W20 buffer: pH 8.0 (50mM sodium phosphate, 1M NaCl, 20mM imidazole, 10% glycerol)
To Make 200 mL:
100mL 2x stock buffer
4mL 1M imidazole *(stored in dark at 4C)*
96mL ddH_2O

Elution Buffer:
W500 buffer: pH 8.0 (50mM sodium phosphate, 1M NaCl, 500mM imidazole, 10% glycerol)
To make 30 mL:
15mL 2x stock buffer
15mL 1M imidazole *(stored in dark at 4C)*

SEC running buffer:
S-300 buffer: pH 8.0 (50mM tris-HCl, 150mM KCl, 1mM DTT, 0.5mM EDTA, 10% glycerol)
To Make 500mL:

Be sure to filter, and degas right before use!
25mL 1M tris-HCL *(stored at RT in chem room)*
37.5mL of 2M KCL
500uL 1M DTT *(stocks stored at -20C) **Add DTT after filtering*
500mL 0.5M EDTA *(stored at RT in chem room)*
50mL glycerol
Add ddH2O to final volume 500mL and adjust pH to 8.0.

Days 1&2:

1. Streak cells onto an amp plate (either from stock or transformed) and grow O/N at 37C.
2. Set up an overnight culture at 37C in LB + Amp media *(5-10mL for each L growth)*.
3. Make buffers on day 2 and store at 4C in cold room.

Day 3:

1. Pre-chill JLA-8.1000 rotor (step 7) to 4C (*York lab)*.
2. Prewarm LB amp media at 30C in shaking incubator, 200-220 rpm.
3. Sub-inoculate O/N cultures and grow to OD600 ~0.5 *(usually 5-10mL culture in each L)*.
4. *Collect an SDS-PAGE sample (step 10)*.
5. Once grown to OD600 ~0.5, induce with 0.5mM IPTG
    a. i.e. for 1M IPTG, ad 500uL in 1L culture.
6. Incubate for 3 hours at 30 (or overnight at 18c) and *collect and SDS-PAGE sample (step 10)*.
7. **Weigh an empty container before pelleting cells. Will be used to calculate cell mass (step 9).*
8. Pellet the cells using the JLA-8.1000 rotor and Beckman Coulter centrifuge (*York Lab)* at 4,000xg for 15 minutes at 4C.
9. Discard supernatant and resuspend pellet in 3mL S buffer per g/cells.
    a. *To resuspend, use either cell scraper and/or plastic pipetman. Mix well to ensure that all is removed from bottle walls.*
10. Transfer to 50mL falcon tubes and flash freeze cells with liquid nitrogen, store at -80C O/N.
11. *SDS-PAGE Samples
    a. Volume of cells = 60 / (OD600 value), pellet cells.
    b. Resuspend pellet in 15uL ddH_2O.
    c. Add 10uL 5x Sample Buffer (2x final concentration) (*in -20C box)*
12. **Consider equilibrating FPLC to water overnight (~0.3mL/min flow over 120 mL).
    a. Use S300-HR 16/60 column. *(York Lab cold room).*

Day 4:

1. Pre-chill JA25.50 rotor (step 6) to 4C (*York Lab)*.
2. Thaw cell slurry in water using a stir plate and thoroughly resuspend *by pipetting*.
3. Lyse cells using microfluidizer, 3 rounds.
4. Transfer homogenized cells to 50mL centrifuge tubes *(stored in alcove)*.
5. *If lysate is too thick, consider adding 500 units nuclease or benzonase. **Do not add PMSF!**

6. Centrifuge cell lysate at 30,000 x g for 30 min at 4C and recover the clarified supernatant.
7. *Collect 10uL of supernatant for SDS-PAGE sample. (+10uL ddH_2O +5uL buffer).*
8. During the spin, equilibrate an appropriate amount of NiNTA resin in S-buffer.
    a. Slurry is 50% resin, e.g. 4mL slurry to get 2mL resin.
    b. Pellet resin by spinning at 750 x g for 5 minutes.
    c. Wash 1x with 5xCV (10mL) H_2O
    d. Wash 3x with 10xCV (20mL) S-buffer.
9. Add clarified lysate to resin in 50mL falcon tubes and incubate for 1hr rotating in cold room.
10. Pellet Resin and remove most of the supernatant *(save supernatant, just in case)*.
11. Resuspend resin in remaining amount of clarified lysate and transfer to plastic column.
12. Wash with 100mL (50xCV) S-buffer and collect and SDS-PAGE sample.
13. Wash with 100mL (50xCV) W20 buffer and collect an SDS-PAGE sample.
14. Elute with 15mL W500 buffer and immediately start collecting fractions.
    a. With 2mL resin, ClpP began to elute at after 1mL.
        i. Test all fractions with 1X Bradford: add 1uL of each fraction to 50uL 1x dye.
    b. Create SDS-PAGE samples of desired fractions to run on a gel (10uL sample/H_2O).
15. Pool desired fractions and concentrate using spin filter down to a little more than 1mL (if bigger loops are available, can increase volume. The column allows <5mL of sample).
    a. Concentrate using an Amicon Ultra-15 10kDa MWCO filters (15mL max volume).
    b. I always spin at 4C, 10-15min at 5000 x g (max allowed speed) concentrates ~2x.
    c. Only spin 15min at a time and mix above filter by pipetting after each spin.
16. **Equilibrate FPLC if running tomorrow (1st in H_2O and then in S-300 buffer, 120mL each (1xCV). Do not exceed 0.15MPa above system back pressure).

Day 5:

1. Pre-clear sample by spinning at max speed for 10min at 4C.
2. Load concentrated sample onto FPLC and collect necessary fractions.
    a. Collect 2mL fractions beginning at the void volume (~36mL)
3. Run fractions on an SDS-PAGE gel to verify purity and select appropriate fractions.
    a. Higher molecular weight proteins not separated too well (see below).
4. Pool desired fractions and concentration using spin concentrator.
    a. *For the prep shown in the appendix, I kept fractions 1-16, 20-26 (~46mL)*.
    b. For a 2L prep, I concentrated down to ~1.5mL, which was at 3.76uM.
5. Determine the concentration using a nanospec (2uL works better for protein). The extinction coefficient is 125,160 $M^{-1}cm^{-1}$ (tetradecamer).
6. Biotinylate according to the specific protocol (depends on the maleimide being used).
    a. I used EZ-Lin Maleimide-PEG2-Biotin. Thermo: 21901BID.

To store the column, run 1CV of H_2O followed by 1CV EtOH.

Expression and Purification of HaloTag-multidomain substrate

Materials:
Production and Expression:
- Amp media plates *(in cold room stock)*
- LB Media (Make fresh beforehand)
- 1000x Ampicillin *(stocks in -20C)*
- 1M IPTG *(stocks in -20C)*
- 12% SDS-PAGE gels (need 5+)

Stock Buffer (2x):
pH 8.0 (100mM sodium phosphate, 1M NaCl, 20% glycerol)
To make 500mL:
3mL of 1M NaH_2PO_4 *(on chemicals shelf)*
94mL of 0.5M Na_2HPO_4 *(on chemicals shelf)*
29.22g NaCl
100mL glycerol
Adjust pH to 8.0 and bring total volume to 500mL.

Lysis Buffer
pH 8.0 (50mM sodium phosphate, 500mM NaCl, 10% glycerol, 10mM BME, 20mM imidazole)
To make 500mL:
250mL stock buffer
10mL of 1M imidazole *(stored in 4C fridge)*
350uL of 14.3M BME *(in chemical hood)*
240mL ddH2O

Elution Buffer
pH 8.0 (50 mM sodium phosphate, 500 mM NaCl, 10% glycerol, 10mM BME, 250mM imidazole)
To make 100mL:
50mL stock buffer
25mL of 1M imidazole *(stored in 4C fridge)*
70uL of 14.3M BME *(in chemical hood)*
25mL ddH2O

SEC running buffer:
pH 7.6 (20 mM Hepes, 200 mM KCl, 0.1 mM EDTA, 1 mM DTT)
To make 500mL:
10mL of 1M Hepes *(stockroom in foil)*
50mL of 2M KCL
100mL 0.5mM EDTA
Adjust pH to 7.6 and final volume to 500mL
Filter sterilize
Add 500uL 1M DTT before use.
Degas right before use on FPLC

Days 1&2:

1. **Be sure to sign up for incubators, FPLC, and York lab centrifuge as necessary!**
2. Streak an amp plate (either from glycerol stock or transformed) and grow at 37C overnight.
3. The next day, set up an overnight culture at 37C in LB + Amp (~5-10mL per L growth).
4. Prepare buffers on day 2 and store in cold room.

Day 3 (Growth and Induction):

1. Prewarm LB + Amp media at 37C in shaking incubator, 200-220 rpm.
2. Sub-inoculate cultures (100-200 fold dilution) and grow to OD600 ~ 0.6.
3. At OD600 ~ 0.6, *Collect an SDS-PAGE sample (step 10)*.
4. Reduce temperature to 25C and induce with 1mM IPTG (i.e. add 1mL of 1M IPTG to 1L LB).
5. Grow cells 3-4 hours and harvest using JLA 8.1000 rotor *(York Lab)* at 4000xg for 15min.
6. Discard supernatant and wash cells in 1x stock buffer.
7. Pellet cells again by spinning at 4000xg for 15min.
8. Discard supernatant and resuspend cell pellets in lysis buffer (10mL per 1g cells).
9. Flash freeze cells and store at -80.
10. *SDS-PAGE samples
    a. Volume of cells = 60 / OD600 value. Spin to pellet cells
    b. Resuspend cell pellet in 15uL H2O.
    c. + 10uL of 5x sample buffer (2x final).

Day 4 (Lysis and affinity chromatography):

1. **Equilibrate S300 column one day in advance. 120mL H_2O then 120mL SEC buffer.
2. Pre-chill JA25.50 rotor to 4C (step 7) *(York Lab)*.
3. Lyse cells using microfluidizer, 3 rounds.
4. Make fresh 1mM PMSF (0.0174g in 1mL isopropanol).
5. Add benzonase (250 units per 200mL lysate) and PMSF (100uL per 100mL lysate) and incubate for ~30min rotating at 4C.
6. Clarify lysate by spinning at 30,000xg for 30min at 4C *(York Lab)*.
7. During the clarification, equilibrate nickel resin (1-2mL per 5g cells):
    a. Pellet resin at 500xg for 5min.
    b. Wash 1x with 5 volumes H_2O (e.g. if using 2 mL resin, 10mL H_2O).
    c. Wash 3x with 10 volumes lysis buffer.
8. Recover the clarified supernatant and *collect a sample for SDS-PAGE (step 24).*
9. Add the clarified lysate to the washed resin in 50mL falcon tubes.
10. Incubate rotating at 4C for ~1Hr.
11. Pellet resin by spinning at 500xg for 5min and remove most (but not all) of the supernatant.
12. Resuspend the pellet in remaining lysate and pour onto column.
13. *Collect flowthrough for an SDS-PAGE sample.*
14. Wash with 50xCV Lysis buffer and *collect an SDS-PAGE sample*.
15. Elute (usually 5mL elution buffer per 1mL resin) and collect ~1mL fractions.
    a. *Create SDS-PAGE samples of desired fractions*.
16. Pool appropriate fractions and concentrate down to ~1-3mL for FPLC (old vs new akta).
    a. Use 10kDa Amicon spin concentrators, 5000xg for 5min each spin.

Day 5 (Size exclusion chromatography):

1. **S300 column should be equilibrated into buffer by today**.
2. Pre-clear sample by spinning at max speed for 10min at 4C.

3. Load samples onto FPLC and collect necessary 2mL fractions (see chromatogram in appendix).
4. Clean column with H_2O and finally EtOH (120mL).
5. Run appropriate fractions on SDS-PAGE to select pure fractions.
    a. If samples remain “dirty” consider ion exchange column.
6. Concentrate sample to desired working concentration (usually 10uM). (ε_{280}= 89,380 $M^{-1}cm^{-1}$).
7. Aliquot as desired (usually 60uL for unfolding protocol) and flash freeze in liquid nitrogen. Store at -80C for future use.

Expression and Purification of His-tagged Ulp1 (SUMO Protease)

Buffers:

2x Stock Buffer: (100mM Sodium Phosphate pH 7.5, 600mM NaCl)
To make 400mL:
66.7mL of 0.5M Na_2HPO_4
6.72mL of 1M NaH_2PO_4
48mL of 5M NaCl

Lysis Buffer: (50mM Sodium Phosphate pH 7.5, 300mM NaCl, 10mM Imidazole)
To make 500mL:
250mL of 2x Stock buffer
5mL of 1M Imidazole
245mL of H_2O

Wash Buffer: (50mM Sodium Phosphate pH 7.5, 300mM NaCl, 20mM Imidazole)
To make 100mL:
50mL of 2x Stock buffer
2mL of 1M Imidazole
48mL of H_2O

Elution Buffer: (50mM Sodium Phosphate pH 7.5, 300mM NaCl, 250mM Imidazole)
To make 50mL:
25mL of 2x Stock Buffer
12.5mL of 1M imidazole
12.5mL of H_2O

SEC buffer: (50mM Tris-HCl pH 8.0, 200mM NaCl, 0.5mM TCEP)
Filter and Degas at the day before!
To make 200mL:
10mL of 1M tris-HCl pH 8.0
8mL of 5M NaCl
200mL of 500mM TCEP (add this day of)

Dialysis buffer: (50mM Tris-HCl pH 8.0, 200mM NaCl, 0.5mM TCEP, 50% glycerol)
To make 40mL:
2mL of 1M Tris-HCl pH 8.0
1.6mL of 5M NaCl
25mL of 80% glycerol
40mL of 500mM TCEP (add day of)

Expression:

1. Pick a single colony from either freshly transformed BL 21(DE3) cells, or from a glycerol stock, and inoculate 20 ml of LB + Kanamycin (Kan). Incubate O/N in the 37°C shaker at ~200rpm
2. Make a 1:100 dilution of O/N culture in 1 liter of LB + Kan and incubate shaking at 37°C.
3. Grow cells until an OD600 ~0.5 is reached.
4. Induce cells with 0.5 mM IPTG and continue to incubate shaking at 37°C for another 3 hours.
5. Harvest cells by centrifugation, resuspend in 4mL per gram of Lysis buffer, and freeze at -80°C

Purification:

1. Thaw cell pellet on ice, mix by pipetting to ensure cells are completely thawed and resuspended.
2. Lyse cells using the microfluidizer, 2-3 passes.
    a. Add 125mL of 200mM PMSF per 25mL lysate on the first pass.
    b. To make 200mM PMSF, dissolve 0.034g in 1mL 100% EtOH.
3. If lysate appears very viscous here, consider incubation with nuclease.
4. Centrifuge lysate at 30,000xg for 30 minutes to pellet cellular debris. Save supernatant.
4. During this spin, equilibrate 1mL of nickel resin per 2L cells in lysis buffer
    a. Wash three times with 10 CV buffer.
    b. Pellet by spinning at 700xg for 5min, remove supernatant, and resuspend in buffer.
5. Add the clarified lysate to the equilibrated resin and incubate rotating at 4C for 1 hour.
6. Pellet resin as in step 4, removing and most (but not all) of the lysate.
7. Resuspend the pellet in a small amount of lysate and flow onto the prepared column.
8. Wash with 20CV of wash buffer.
9. Elute protein with 10CV and collect 1mL fractions.
10. Analyze fractions by SDS-PAGE. If clean enough here, pool and aliquot (see step 14).
11. If the fractions are not clean enough, pool and concentrate appropriate fractions and run on the Superdex75.
    a. Max pre-column pressure 2.6 MPa, max flowrate 0.8mL/min, max load 500mL.
12. Analyze appropriate fractions by SDS page.
    a. Protein should come off around 12mL retention volume.
13. Pool appropriate fractions, concentrate, and dialyze into 50% glycerol (dialysis buffer).
    a. If using dialysis device, dialyze once again 14mL for 2Hr, replace with a fresh 14mL and leave rocking gently at 4C overnight.
14. Protease may be stored at –80°C in 50% glycerol, 20mL aliquots at ~300mM.

Molecular Weight: 26829.5 Da
Extinction Coefficient: 28950 M-1cm-1
pI: 6.79

Carboxymethylation of Halo-4I27-ssrA

(Adrian Olivares, Baker Lab, MIT)

Unfolding Buffer (V_T = 50 mL)

100 mM bicine pH 8.8	0.816 g (FW=163.2 g/mol)
8 M guanidine HCL	38.212 g (FW=95.53 g/mol)

Bring up with ddH_2O
pH solution and 0.2 µm filter

Dialysis Buffer (V_T = 250 mL)

20 mM Hepes pH 7.6	10 mL (0.5 M stock)
200 mM KCl	25 mL (2 M stock)
10% glycerol	25 mL
0.1 mM EDTA	50 mL (0.5 M stock)
1 mM DTT	0.25 mL (1 M stock)

Bring up with ddH_2O

PROCEDURE

1) Mix the following:
25 µL Unfolding Buffer
15 µL ddH_2O
60 µL Halo-4I27-ssrA (10 µM stock, V15P variant of I27)
incubate at RT for 1.5 hours

2) Make a fresh 0.5 M stock of iodoacetic acid (FW = 185.95 g/mol) in 1 N NaOH (1 mL 1 N NaOH and 0.093 g iodoacetic acid)

3) Add 0.5 µL iodoacetic acid stock to Halo-4I27-ssrA unfolding reaction (2.5 mM) and incubate at RT for another 1.5 hours covered in foil

4) Quench reaction with 10 mM DTT

5) Dialyze carboxymethylated-Halo-4I27-ssrA against Dialysis Buffer O/N at 4°C

6) Spin down max speed in cold room centrifuge 10 min

7) Measure concentration in 6M guanidine (ε_{280} = 89,380 M^{-1} cm^{-1})

8) Measure Trp fluorescence in fluorimeter (λ_{ex} = 280 nm, λ_{em} = 300-400 nm). There is a characteristic red shift in CM-I27 Trp fluorescence compared to folded protein.

9) Measure Halo binding to Halo-TMR ligand by fluorescence polarization anisotropy ((λ_{ex} = 555 nm, λ_{em} = 585 nm). I used 50 nM ligand and 500 nM Halo protein in buffer of your choosing.

PCR of amine-DNA-biotin

(Olivares Laboratory, Vanderbilt 2017)

Labeled 3500-bp DNA will be used to attach glass binding peptide or HaloTag alkane ligand for single-molecule optical trapping experiments.

primers
OLI007.F: Biotin-M13mp18-3500: /5BiosG/AATCCGCTTTGCTTCTGAC (biotin)
OLI008.R: Amine-M13mp18-3500: /5AmMC6/TTGAAATACCGACCGTGTG (amine)

template
m13mp18 ds DNA plasmid (Bayou Biolabs, Cat # P-105)

reaction mix (V_t = 850 µL)

ddH_2O		561 µL
5X GC buffer		170 µL
10 mM dNTPs	17 µL	
10 µM biotin primer		42.5 µL
10 µM amine primer		42.5 µL
50 ng/µL template		8.5 µL
2000 U/mL Phusion HF DNA polymerase	8.5 µL	

*add polymerase last
*aliquot 50 µL in 2X 8-tube PCR strips
*do not use Hot Start Phusion

PCR cycle

1) 98°C	30 sec
2) 98°C	5 sec
3) 62°C	10 sec
4) 72°C	1 min
5) go to step 2 and repeat 34 times	
6) 72°C	5 min
7) 10°C	hold

Clean up on 2 NucleoSpin columns (Macherey-Nagel) manufacturer's protocol for PCR cleanup
- add 1.7 mL NTI buffer to 850 µL reaction and split into 2 columns (600 µL at a time)
- spin 11000 x g 30 sec
- wash with 700 µL NT3 buffer and spin 11000 x g 30 sec, discard FT and repeat wash
- spin dry 11000 x g 1 min
- add 30 µL PBS (50 mM $NaPO_4$ + 150 mM NaCl, pH 8) to each column, let sit 1 min, spin 1 min

Halotag ligand conjugation

This protocol describes how conjugate halotag ligand to DNA with a free amine via a succinimidyl ester.

Materials:
DNA with free amine label (either oligo or PCR product)
Halotag succinimidyl ester ligand O4 (100mM aliquots in -80C, 5uL)
10x PBS pH 8.0

*** The DNA to be used should not be resuspended in tris buffer (i.e. any of the elution buffers). If it is, you will need to buffer exchange into water or PBS. The free amine on tris will compete with the DNA for the succinimidyl ester.***

Protocol:

1. Mix DNA, succinimidyl ester, 10x PBS, and H2O to final volume 200uL (2.5mM halotag ligand).
    a. e.g. 30uL DNA
    b. +20uL 10x PBS
    c. +5uL succinimidyl ester
    d. +145uL H_2O
2. Incubate at room temp in foil for ~4 Hrs.
3. Optional quenching with 25mM tris-HCl (5uL of 1M).
4. Purify labeled DNA using the appropriate spin column (depends on size of DNA).
    a. For 20bp oligo, I use a Zeba spin desalting column.
    b. If using a larger labeled DNA use QIAquick PCR clean up followed by illustra S400.

Additional protocols:

Zymo DNA/RNA spin columns, buffer exchange:

*Use to buffer exchange oligos if resuspended in tris. ***There are 2 different spin columns, be sure to start with II and then I !****

1. Add 2x volume binding buffer to oligo, add to column II and spin 13,000xg for 1 min. **Keep the FT.**
    a. I used 7uL of 100mM oligo for two spin columns (check binding capacity to be sure).
2. Add same volume etOH to the FT and load onto spin column I.
    a. E.g. I added 21uL here.
3. Spin 13,000xg for 1 min and discard FT.
4. Add 400uL prep buffer and spin, discard FT.
5. Add 700uL wash buffer and spin, discard FT. Repeat for total 2 washes.
6. Spin columns at 13,000xg for 2 min to dry clumn.
7. Elute into 15uL of provided H_2O (nuclease free), 10,000xg for 1 min.

Zeba spin protocol:

1. Vortex column to resuspend resin, twist off the bottom and loosen the cap.
2. Spin at 1,500xg for 1 min.
3. Add 300uL of desired buffer (PBS or 1x PD) and spin at 1,500xg for 1min. Repeat 2 times.
4. Add sample to the column and spin at 1,5000xg for 2min.

Clp(A)P Trapping Protocol

This protocol describes how to prepare beads and buffers for optical trapping Clp(A)P experiments.

Materials:

4x PD buffer (100 mM Hepes pH 7.6, 400 mM KCl, 40% glycerol, 40 mM MgCl2, 2 mM TCEP, 0.4% tween-20)
40 mg/mL BSA
50x Oxygen Scavenger (12.5 mg/mL glc oxidase, 1.5 mg/mL catalase)
50x Glucose (150mg/mL in H_2O)
ClpP, ClpA (if using)
1.2mM ADEP1 (20x in DMSO)
3500bp with overhang (See trapping PCR protocol)
20bp oligo:Halotag ligand (see conjugation protocol)
(CM)-Titin or other substrate protein

Buffers to prepare:

1x PD, 1x PD-BSA-Oxy, 1x PD-BSA-Oxy with ADEP1 (if using)
Only add glucose to the oxygen scavenger system buffers right before use! enzymes acidify solutions over time.
To make 1mL of any of these:

- 250uL 4x PD buffer
- 25uL of 40mg/mL BSA
- 20uL of 50x oxygen scavenger
- 20uL of glucose solution (150mg/mL)
- 50uL of 1.2mM ADEP1
- H_2O up to 1mL (depending on components added)

Protocol:

Note: Some of the next steps can be done at the same time. They are split up into sections to help understanding.

Generally, it's a good idea to load >300uL of solution into the syringes on the trap. You may change volumes if needed, as long as final volume will not be too much lower. With the oxygen scavenger system, you can probably get ~2-3 hrs of good trapping time before "weird" things start happening (at least for ClpP experiments in my hands).

Washing streptavidin beads:

1. Mix 10uL of bead solution and 90uL of 1x PD buffer.
2. Pellet beads by spinning at max speed for 1 min.
3. Remove supernatant and wash with 100uL of 1x PD buffer.
4. Repeat steps 2-3 twice (total three washes).
5. Final resuspension into 20uL of 1x PD.

Preparation of substrate beads:

Still might be testing 3500bp DNA amount here…

1. Add an ~equimolar amount of halotag ligand to substrate.
    a. E.g. 1uL of 353ng/uL oligo to 35uM CM-Titin (10uL aliquot).
2. Incubate at room temp (~22C) in foil for 1 hour.

3. Meanwhile incubate 10uL of beads from previous step with 5uL 3500bp DNA (300ng/uL), rotating at room temp for ~30min.
4. Pellet substrate beads and resuspend in appropriate volume (7uL) of H_2O.
5. Set up a ligation reaction to ligate substrate to 35000bp DNA.
    a. Mix 7uL 3500bp beads.
    b. + 11uL substrate:oligo:halotag ligand
    c. + 2 uL 10X T4 ligase buffer
    d. + 1 uL T4 ligase
6. Incubate rotating at room temp > 10min.
7. Pellet beads by max speed spin 1 min.
8. Wash beads once with 50uL 1x PD buffer.
9. Final resuspension in 1x PD-BSA with oxygen scavenger system.

Preparation of ClpP Beads:
Still might be testing [ClpP] here.

1. Add 2uL of 3.4uL ClpP:biotin to 10uL of beads from step 1 (~560nM)
2. Add 0.6uL of 1.2mM ADEP1 to this bead solution.
3. Incubate rotating at room temp for ~30min.
4. Pellet beads and wash once with 1x PD-BSA-Oxy with ADEP.
5. Final resuspension 50uL.

Dilution for optical trap:
This dilution can depend on how much material you lost during each of the washes. If worried, start with a 1:10 dilution and flow solution onto trap to check density.

1. Take 25 uL of bead solution and add 375uL (400uL total).
2. Keep the remaining volume of beads and buffers on ice in the dark until loaded onto the trap.

The way I have been setting it up on the trap:
Channel 1 – substrate beads
Channel 2 – 1x PD-BSA-oxy -ADEP
Channel 3 – 1x PD-BSA-oxy -ADEP
Channel 4 – 1x buffer + ADEP
Channel 5 – ClpP beads

Lifetime script

This script controls the LUMICKs optical trap to perform lifetime experiments.

```
# -*- coding: utf-8 -*-
"""
Rupture forces for Clp(A)P

@author: Steven Walker
"""
import sys
import bluelake
from bluelake import trap1, trap2, stage, pause, timeline, reset_force, fluidics


#Variables to change for each experiment.
bead_threshold = 85             #Desired match score threshold
force_threshold = 4.5           #pN force to "sense" a tether
minimum_distance = 0.35         #Closest point during fishing
maximum_distance = 1.6          #Farthest point during fishing
dwell_time = 3                  #Seconds to wait ends during fishing
bead_channel = 'beads'          #Channel name for beads
tether_channel = 'DNA'          #Channel name for molecules of interest
buffer_channel = 'buffer'       #Channel name for experiments
junction = 'J1'                 #Name of location to capture bead in trap1.
pull_force = 15


force_break = False
def catch_2_beads(threshold, channel_1, channel_2,channel_3):
    """This function will catch two beads according to desired score."""
    traps = [trap1, trap2]
    score1 = timeline['Tracking Match Score']['Bead 1']
    score2 = timeline['Tracking Match Score']['Bead 2']
    scores = [score1, score2]

    for trap in traps:
        trap.clear()

    stage.move_to(channel_1)

    while score1.latest_value < threshold:
        if any(0 < s.latest_value < threshold for s in scores):
            for trap in traps:
                trap.clear()
            pause(1)

    stage.move_to('JM',speed=50)
    pause(3)
    stage.move_to(channel_2, speed=50)
    #stage.move_to(channel_3, speed=25)

    trap1.clear()
```

```
    if score1.latest_value < threshold:
        print('First bead was lost \n Start the program again')
        sys.exit('First bead was lost')


    trap1.move_to(x=71, speed=10)

    while score2.latest_value < threshold:
        if 0 < score2.latest_value < threshold:
            trap1.clear()
            pause(1)


def goto_distance(target, threshold):
    """Moves trap 1 to desired starting position away from trap 2 (according
    to the target input)."""
    global force_break
    distance = timeline['Distance']['Distance 1']
    delta_x = distance.latest_value - target

    while abs(delta_x) > 0.01:
        if trap2.current_force > threshold:
            force_break = True
            print(force_break)
            break
        elif delta_x <=0:
            trap1.move_by(dx= +0.1) #ping pong speed
        else:
            trap1.move_by(dx = -0.03)
        delta_x = distance.latest_value - target


def fishing(min_distance, max_distance, wait, threshold):
    """Fishes for a tether between the two captured beads."""
    global force_break
    goto_distance(min_distance,4*threshold)
    pause(wait)
    counter = 0
    while counter <=4:
        goto_distance(max_distance/2,4*threshold)
        goto_distance(max_distance,threshold)
        if force_break == True:
            break
        goto_distance(min_distance,4*threshold)
        pause(wait)
        counter+=1
        if counter ==4:
            print('No tether found, start script again')
            sys.exit()
        print(counter)
```

```
def pull_to_force(target):
    """Moves trap1 until target force is reached, waits until rupture by
    checking force value every second."""
    distance = timeline['Distance']['Distance 1']
    pause(1)
    while abs(trap2.current_force) < target:
        trap1.move_by(dx=+0.05)         #0.005 = 55nm/s
        pause(0.025)
        if distance.latest_value >= 3:
            break
    while abs(trap2.current_force) > 1:
        pause(0.5)


#Making a counter to automate marking
if not hasattr(bluelake, 'marker_count'):
    bluelake.marker_count = 0

#These lines control the script by calling the functions above.
while fluidics.pressure<0.04:       #Increasing presure up to 0.1 bar.
    fluidics.increase_pressure()
catch_2_beads(bead_threshold, bead_channel, junction, tether_channel)   #First catches two
beads
print('Beads caught')
stage.move_to('JM',speed=25)
pause(3)
stage.move_to('Ch1', speed=50)
pause(8)
stage.move_to(buffer_channel, speed=25)
pause(5)
fluidics.stop_flow()
if timeline['Tracking Match Score']['Bead 2'].latest_value ==0:
    print('Second bead was lost \n Start the program again')
    sys.exit()
                    #Moves to buffer channel
pause(2)
fluidics.stop_flow()
trap1.move_to(x=35.5, speed=9)                              #Moving to 1.5um to zero force
fluidics.stop_flow()                                        #Stops flow for exp.
#stage.move_to('J1', speed=30)
#stage.move_to('Ch1', speed=50)
goto_distance(1.6, 3*force_threshold)
pause(3)
reset_force()
pause(1)
print('Starting to fish')
#while fluidics.pressure<0.04:       #Increasing presure up to 0.1 bar.
    #fluidics.increase_pressure()
fishing(minimum_distance, maximum_distance, dwell_time, force_threshold)
goto_distance(maximum_distance/2, 4*force_threshold)
#fluidics.stop_flow()
```

```
#pause(2)
#fluidics.stop_flow()
print('Tether is present, beginning experiment')
timeline.mark_begin('lifetime at {} no {}'.format(pull_force,bluelake.marker_count))
pull_to_force(pull_force)                                    #Executing pull to specific force
pause(2)
trap1.move_to(x=35.5, speed=1)
pause(1)
goto_distance(1.5,force_threshold*10)                        #Ensuring the trap moves to 1.5 microns
after rupture
print('Waiting for baseline')
pause(2)                                                     #Waiting 5s for ending baseline.
timeline.mark_end()
print('Experiment finished!')
bluelake.marker_count +=1
```

Rupture Force Script

This script controls the LUMICKs optical trap to perform rupture force experiments.

```
# -*- coding: utf-8 -*-
"""
Rupture forces for Clp(A)P

@author: Steven Walker
"""
import sys
import bluelake
from bluelake import trap1, trap2, stage, pause, timeline, reset_force, fluidics


#Variables to change for each experiment.
bead_threshold = 90            #Desired match score threshold
force_threshold = 4.5          #pN force to "sense" a tether
minimum_distance = 0.45        #Closest point during fishing
maximum_distance = 1.6         #Farthest point during fishing
dwell_time = 8                 #Seconds to wait ends during fishing
bead_channel = 'beads'         #Channel name for beads
tether_channel = 'DNA'     #Channel name for molecules of interest
buffer_channel = 'buffer'      #Channel name for experiments
junction = 'J1'                #Name of location to capture bead in trap1.
step_size = 0.02               #0.005 = 55nm/s


force_break = False
def catch_2_beads(threshold, channel_1, channel_2,channel_3):
    """This function will catch two beads according to desired score."""
    traps = [trap1, trap2]
    score1 = timeline['Tracking Match Score']['Bead 1']
    score2 = timeline['Tracking Match Score']['Bead 2']
    scores = [score1, score2]

    for trap in traps:
        trap.clear()

    stage.move_to(channel_1)

    while score1.latest_value < threshold:
        if any(0 < s.latest_value < threshold for s in scores):
            for trap in traps:
                trap.clear()
            pause(1)

    stage.move_to('JM',speed=50)
    pause(3)
    stage.move_to(channel_2, speed=50)
    #stage.move_to(channel_3, speed=25)
```

```
    trap1.clear()
    if score1.latest_value < threshold:
        print('First bead was lost \n Start the program again')
        sys.exit('First bead was lost')


    #pause(10)

    trap1.move_to(x=70, speed=10)
    #pause(2)

    while score2.latest_value < threshold:
        if 0 < score2.latest_value < threshold:
            trap1.clear()
            pause(1)


def goto_distance(target, threshold):
    """Moves trap 1 to desired starting position away from trap 2 (according
    to the target input)."""
    global force_break
    distance = timeline['Distance']['Distance 1']
    delta_x = distance.latest_value - target

    while abs(delta_x) > 0.01:
        if trap2.current_force > threshold:
            force_break = True
            print(force_break)
            break
        elif delta_x <=0:
            trap1.move_by(dx= +0.01)
        else:
            trap1.move_by(dx = -0.03)
        delta_x = distance.latest_value - target


def fishing(min_distance, max_distance, wait, threshold):
    """Fishes for a tether between the two captured beads."""
    global force_break
    goto_distance(min_distance,3*threshold)
    pause(wait)
    counter = 0
    while counter <=4:
        goto_distance(max_distance/2,2.5*threshold)
        goto_distance(max_distance,threshold)
        if force_break == True:
            break
        goto_distance(min_distance,4*threshold)
        pause(wait)
        counter+=1
        if counter ==4:
```

```
            print('No tether found, start script again')
            sys.exit()
        print(counter)

def pull_to_rupture(step_size):
    """Moves trap1 until target force is reached, waits until rupture by
    checking force value every second."""
    distance = timeline['Distance']['Distance 1']
    pause(1)
    while distance.latest_value < 3:
        trap1.move_by(dx=step_size)         #0.005 = 55nm/s
        if trap2.current_force <0.3:
            break
        elif distance.latest_value >= 3:
            break



#Making a counter to automate marking
if not hasattr(bluelake, 'marker_count'):
    bluelake.marker_count = 0

#These lines control the script by calling the functions above.
while fluidics.pressure<0.04:       #Increasing presure up to 0.1 bar.
    fluidics.increase_pressure()
catch_2_beads(bead_threshold, bead_channel, junction, tether_channel)   #First catches two
beads
print('Beads caught')
stage.move_to('JM',speed=25)
pause(3)
stage.move_to('Ch1', speed=50)
pause(10)
stage.move_to(buffer_channel, speed=25)
pause(5)
if timeline['Tracking Match Score']['Bead 2'].latest_value ==0:
    print('Second bead was lost \n Start the program again')
    sys.exit()
                #Moves to buffer channel
pause(2)
fluidics.stop_flow()
trap1.move_to(x=35.6, speed=9)                          #Moving to 1.5um to zero force
fluidics.stop_flow()                                    #Stops flow for exp.
#stage.move_to('J1', speed=30)
#stage.move_to('Ch1', speed=50)
goto_distance(1.5, 3*force_threshold)
pause(3)
reset_force()
pause(1)
print('Starting to fish')
fishing(minimum_distance, maximum_distance, dwell_time, force_threshold)
goto_distance(maximum_distance/2, 4*force_threshold)
```

```
print('Tether is present, beginning experiment')
timeline.mark_begin('{} rupture force {}'.format(step_size,bluelake.marker_count))
pull_to_rupture(step_size)                          #Executing pull to specific force
pause(2)
trap1.move_to(x=35.6, speed=1)
pause(1)
goto_distance(1.5,force_threshold*10)               #Ensuring the trap moves to 1.5 microns
after rupture
print('Waiting for baseline')
pause(2)                                            #Waiting 5s for ending baseline.
timeline.mark_end()
print('Experiment finished!')
bluelake.marker_count +=1
```

Subplots

This script creates three graphs of all the .h5 files in a given directory. It saves them in a directory named figures within the directory with the data.

```
# -*- coding: utf-8 -*-
"""
This script is used to create 3 plots from a .h5 file. It plots Force vs. Time,
distance vs. Time, and then Force vs. Distance. This will be helpful in
identifying which experiments were done properly and had only 1 tether.

@author: walke
"""
from os import listdir,mkdir
from os.path import isfile, join, exists
from lumicks import pylake
import matplotlib.pyplot as plt
import math


directory_name = '2021-12-15 ADEP ClpPS97A ruptures (200nms)'          #Folder where all
.h5 files are.

#Creating data frame with Force and distance from .h5 files in folder.
#This line creates a list with all .h5 file names.
filenames = [f for f in listdir(directory_name) if isfile(join(directory_name, f))]
divide = '/'
colors = ['r','g','b','m','c','k']
for name in filenames:
    #This loop iterates through filenames to retrieve force and data from each .h5 file.
    file =pylake.File(divide.join([directory_name,name]))
    hf_force = file.force2x.data
    hf_timestamps = file.force2x.timestamps
    lf_force = file.downsampled_force2x.data
    lf_timestamps = file.downsampled_force2x.timestamps
    distance = file.distance1.data
    hf_time = (hf_timestamps-hf_timestamps[0])/1e9
    lf_time = (lf_timestamps - lf_timestamps[0])/1e9
    data_700 = file.force2x.downsampled_by(50)
    force_700 = data_700.data
    time_700 = (data_700.timestamps-data_700.timestamps[0])/1e9
    data_50 = file.force2x.downsampled_by(700)
    force_50 = data_50.data
    time_50 = (data_50.timestamps - data_50.timestamps[0])/1e9

    #Creating figure with 3 subplots.
    plt.style.use('ggplot')
    f,axs=plt.subplots(1,3,figsize=(16,8))
    portion_700=math.ceil(len(time_700)/6)
    portion_50=math.ceil(len(time_50)/6)
    portion_lf=math.ceil(len(lf_time)/6)
    for i in range(5):
        if i<4:
```

```
            axs[0].plot(time_700[i*portion_700:(i+1)*portion_700],
force_700[i*portion_700:(i+1)*portion_700], '0.8')

axs[0].plot(time_50[i*portion_50:(i+1)*portion_50],force_50[i*portion_50:(i+1)*portion_50],c=colo
rs[i])

axs[1].plot(lf_time[i*portion_lf:(i+1)*portion_lf],distance[i*portion_lf:(i+1)*portion_lf],c=colors[i])

axs[2].plot(distance[i*portion_lf:(i+1)*portion_lf],lf_force[i*portion_lf:(i+1)*portion_lf],colors[i])
        else:
            axs[0].plot(time_700[i*portion_700:], force_700[i*portion_700:], '0.8')
            axs[0].plot(time_50[i*portion_50:],force_50[i*portion_50:],c=colors[i])
            axs[1].plot(lf_time[i*portion_lf:],distance[i*portion_lf:],c=colors[i])
            axs[2].plot(distance[i*portion_lf:],lf_force[i*portion_lf:],colors[i])

    #Adding axis and graph titles.
    axs[0].set_xlabel('Time (s)', size=16)
    axs[0].set_ylabel('Force (pN)', size=16)
    axs[0].tick_params(labelsize=12)
    axs[0].set_title('Force vs Time', size=18)
    axs[1].set_xlabel('Time (s)',size = 16)
    axs[1].set_ylabel('Distance (um)',size=16)
    #axs[1].set_ylim(np.median(distance)-0.1,np.median(distance)+0.1)
    axs[1].tick_params(labelsize=12)
    axs[1].set_title('Distance vs Time', size=18)
    axs[2].set_xlabel('Distance (um)',size=16)
    axs[2].set_ylabel('Force (pN)',size=16)
    axs[2].tick_params(labelsize=12)
    axs[2].set_title('Force vs Distance',size=18)
    if exists('{}/Figures'.format(directory_name))==True:
        plt.savefig('{}/Figures/{}png'.format(directory_name,name[:-2]))
    else:
        mkdir('{}/Figures'.format(directory_name))
        plt.savefig('{}/Figures/{}png'.format(directory_name,name[:-2]))
    plt.close()

#To get stiffness
#name = file['Calibration']['#']['Force 2x']
#stiff = name.h5.attrs.get('kappa (pN/nm)')
#for trap position measurements -0.3734
```

All Ruptures

This code contains a function that finds ruptures by looking at the first derivative of the data. This function is called by the lifetime script that follows. If ran alone, it will find all the ruptures for each .h5 file in a given directory and save them to an excel file.

```
# -*- coding: utf-8 -*-
"""
All ruptures
This script will find the rupture point for all files within a given folder.

@author: walke
"""
from os import listdir, mkdir
from os.path import isfile, join, exists
from lumicks import pylake
import pandas as pd
import matplotlib.pyplot as plt
import numpy as np


directory_name = '2021-08-18 ADEP ClpPS97A'         #Folder name with all .h5 files.
rupture_threshold= 5                                #Force threshold to find a rupture.


def find_rupture(force,threshold):
    """This function is called to find the rupture force. It uses the difference
    vector to spot the point of rupture, and then searches for the maximum within
    5 points. This is to cover the possibility of intermediates (possibly slipping)"""
    # force = force - min(force)                #Subtracting 0 force, need to fix in future
    differences = np.diff(force)                #Differences to find rapid changes
    ruptures = np.where(differences <-1*threshold)   #Getting indeces below threshold
    if len(ruptures[0]) ==0:
        return(False)
    else:
        return(ruptures[0][0])

if __name__ == '__main__':
    #getting file names
    plt.style.use('ggplot')
    filenames = [f for f in listdir(directory_name) if isfile(join(directory_name, f))]
    divide = '/'
    columns = ['Distance','Force']
    Data = pd.DataFrame(columns=columns)
    ruptures = []
    for name in filenames:
        file =pylake.File(divide.join([directory_name,name]))
        data_1000 = file.force2x.downsampled_by(35)
        force_1000 = data_1000.data
        time_1000 = (data_1000.timestamps-data_1000.timestamps[0])/1e9
        distance = file.distance1.data
        force= file.downsampled_force2x.data
```

```
        time=file.downsampled_force2x.timestamps
        time=(time-time[0])/1e9
        #Data = Data.append({columns[0]:distance,columns[1]:force},ignore_index=True)

        index = find_rupture(force,rupture_threshold)   #This will be used as a mask to find rupture
forces.

        if index == False:
            print('bad trace')
            ruptures.append(0)
            continue
        ruptures.append(force[index])       #This list will be populated with the rupture forces.
    # for i in range(len(Data)):
    #     index.append(find_rupture(Data['Force'][i],rupture_threshold))

    # for i in range(len(Data)):
    #     if index[i] == [np.nan]:
    #         pass
    #     else:
    #         for j in range(len(index[i])):
    #             ruptures.append(Data['Force'][i][(index[i][j])])

        plt.figure()
        plt.plot(time_1000,force_1000,'0.8')
        file.downsampled_force2x.plot()
        plt.plot(time[index],force[index],'bo',markersize=15)
        plt.title('{}'.format(name[14:]))
        # plt.close()



    #Making histogram of all rupture forces found.
    plt.figure()
    plt.hist(ruptures, bins=np.arange(0,round(max(ruptures)),5))
    plt.xlabel('Force (pN)')
    plt.ylabel('Frequency')
    plt.title('Rupture Forces')
    export_times = pd.DataFrame(ruptures)

    # if exists('{}/Figures'.format(directory_name))==True:
    #
export_times.to_excel('{}/Figures/{}_Rupture_Forces.xlsx'.format(directory_name,directory_nam
e[:10]))
    # else:
    #     mkdir('{}/Figures'.format(directory_name))
    #
export_times.to_excel('{}/Figures/{}_Rupture_Forces.xlsx'.format(directory_name,directory_nam
e[:10]))
```

Modified Lifetimes

This script finds the lifetime of a tether at a target force by using ruptures to find the end point and by examining the second derivative to find the initial point. It does this for all .h5 files in a given directory and saves them to an excel file within the figures directory.

```
# -*- coding: utf-8 -*-
"""
Created on Wed Nov  3 11:56:19 2021

@author: walke
Modified lifetime script, using 2nd derivative to find starting point.
"""
from lumicks import pylake
import matplotlib.pyplot as plt
import numpy as np
from all_ruptures import find_rupture
from os.path import isfile, join, exists
from os import listdir, mkdir
import pandas as pd

directory_name = '2021-12-07 ADEP ClpP wt lifetimes'
rupture_threshold = 2                #(pN) Force difference defined as rupture.

#Moving mean function using cumsum.
def moving_mean(x,N):
    cumsum = np.cumsum(np.insert(x,0,0))
    return ((cumsum[N:]-cumsum[:-N])/float(N))[::N]

filenames = [f for f in listdir(directory_name) if isfile(join(directory_name, f))]
divide = '/'
times = []
average_force=[]
#columns = ['Distance','Force','Time']
#Data = pd.DataFrame(columns=columns)
for name in filenames:
    file =pylake.File(divide.join([directory_name,name]))
    data_1000 = file.force2x.downsampled_by(35)
    force_1000 = data_1000.data
    time_1000 = (data_1000.timestamps-data_1000.timestamps[0])/1e9
    distance = file.distance1['1s':].data
    force= file.downsampled_force2x['1s':].data
    force_avg = moving_mean(force, 5)
    time=file.downsampled_force2x['1s':].timestamps
    time=(time-time[0])/1e9+1
    time_avg = moving_mean(time, 5)

    deriv1 = np.diff(force_avg)
    deriv2 = np.diff(deriv1)
    start = np.where(deriv2 < -0.5)
    if len(start[0])==0:
        print('Bad Trace')
```

```
        times.append(0)
        average_force.append(0)
        continue
    index_start = start[0][0]+1


    index_end = find_rupture(force_avg,rupture_threshold)          #using find_rupture --> how do I
do this in python again?

    if index_end == [np.nan] or index_end == index_start:
        print('Bad trace')
        times.append(0)
        average_force.append(0)
        continue
    #Plotting ruptures on a force vs time plot.
    plt.style.use('ggplot')
    plt.figure()
    plt.plot(time_1000,force_1000,'0.8')
    plt.plot(time_avg,force_avg)
    plt.plot(time_avg[index_start],force_avg[index_start],'bo',markersize=15)
    plt.plot(time_avg[index_end],force_avg[index_end],'bo',markersize=15)
    plt.title('{}'.format(name[14:]))

    #This is giving how much time elapsed between reaching target force and rupture.
    time_to_rupture=time_avg[index_end]-time_avg[index_start]
    mean_force= np.mean(force_avg[index_start:index_end])
    times.append(float(time_to_rupture))
    average_force.append(float(mean_force))
    print('The tether lasted {} seconds at target force'.format(time_to_rupture))

plt.figure()
plt.hist(times)#bins=np.arange(0,round(max(times)[0]),5))
export_times = pd.DataFrame({ "Force":average_force, 'Lifetimes':times})

if exists('{}/Figures'.format(directory_name))==True:

export_times.to_excel('{}/Figures/{}_Lifetimes_new.xlsx'.format(directory_name,directory_name[
:10]))
else:
    mkdir('{}/Figures'.format(directory_name))

export_times.to_excel('{}/Figures/{}_Lifetimes_new.xlsx'.format(directory_name,directory_name[
:10]))
```